SLAC-PUB-501
September 1968
(EXP)

TWO-BODY PHOTOPRODUCTION*

B. Richter
Stanford Linear Accelerator Center
Stanford University, Stanford, California

(Rapporteur's Report presented at the XIVth International Conference on High Energy Physics, Vienna, August 28 — September 5, 1968)

*Work supported by the U. S. Atomic Energy Commission.

As is usual at these conferences, too much material has been submitted to allow a complete summary of all new photoproduction data in this report. I have therefore restricted myself to summarizing those works which bear most immediately on the problems of strong interaction physics. This means that I will report almost exclusively on high energy experiments and will regretfully omit much very nice work in the region of the resonances.

I. Charged Single-Pion Photoproduction

A. π^+ Production from the Proton

New data are available from my group at SLAC[1] which gives increased accuracy and extends the momentum transfer range of the results which have been previously reported.[2] These new results, together with the old SLAC data and some of the DESY data,[3] are shown in Fig. 1. The main characteristics of these data are the by now well-known spike in the forward differential cross section for momentum transfers less than m_π^2, a t dependence of $\sim e^{2.5t}$ out to momentum transfers of 0.6 GeV^2 followed by a change in slope and a t dependence of $\sim e^{3t}$ out as far as the measurements extend. Figure 2 shows the data on an expanded scale where $(S - M^2)^2 \frac{d\sigma}{dt}$ is plotted vs $(|t|)^{1/2}$ (S is the square of the total center-of-mass energy and M is the proton mass). The new data points are shown in black and the error bars are omitted from the old forward points to reduce confusion on the graph. (The error bars on the old points are larger than those on the new.) The previous data indicated what might have been a systematic trend toward a decrease in the forward differential cross section with increasing energy, although the errors made this conclusion quite uncertain. The new data show that this trend, if present at all, is very much smaller than had been allowed by the previous data. The upper curve shows the yield to be

expected from the electric Born approximation with no absorption. It is interesting to note how close the data come to the Born approximation cross section at 0^{o}. The lower curve indicates the momentum transfer dependence to be expected from models based solely on any combination of evasive Reggeized particle exchange.[4] The peaks in the forward π^{+} photoproduction cross section and in the np charge exchange cross section constitute an insurmountable barrier for any such simple version of the Regge models.

The energy dependence of the differential cross section at fixed momentum transfer was obtained by fitting the data to the form

$$\frac{d\sigma}{dt} = f(t)(S - M^2)^{2\alpha-2} \quad , \qquad (1)$$

where S is the square of the total energy in the center-of-mass system and M is the proton mass. The quantity α in Eq. (1) should not be confused with the Regge trajectory for any given particle. α in Eq. (1) represents an effective energy dependence for the entire cross section. The SLAC data at 8 GeV and above have been used in this fit. The lower energy data have been excluded because of the qualitative difference between the slope of the differential cross section vs momentum transfers for $|t|<0.6$ above and below 8 GeV. Inclusion of lower energy data would systematically decrease α. Figure 3 shows α vs t. The new points are shown as open circles. α remains at or near zero out to $-t \approx 1$ GeV^2. α seems to decrease at $-t = 1.3$ and to return to near zero at $-t = 2$.

B. π^- Production from the Neutron

Since the electromagnetic current possesses both isotopic spin zero and one components, any photoproduction amplitude can be broken up into isotopic vector and isotopic scalar parts. Study of π^- photoproduction from the neutron

and π^+ photoproduction from the proton allows us to learn something about the interference between the isovector and isoscalar parts of the amplitude. The cross sections for π^+ production from the proton and π^- production from the neutron may be written as

$$\frac{d\sigma}{dt}\ (\gamma p \to \pi^+ N) = |A_v + A_s|^2 \qquad (2a)$$

$$\frac{d\sigma}{dt}\ (\gamma N \to \pi^- p) = |A_v - A_s|^2 \ , \qquad (2b)$$

where the subscripts v and s refer to the isovector and isoscalar parts of the amplitude, respectively. Note that this does not refer to the isospin of any exchange particles. All exchange mesons in charged pion photoproduction have an isospin of 1. At high energies an isovector-isoscalar interference term will occur only if there are at least two exchanges in the t-channel having opposite G parity and both belonging to either natural parity ($P = -1^J$) or unnatural $\left[P = -(-1^J)\right]$ sequences.

A group from DESY[5] and my group at SLAC[6] in contributions to this Conference have described experiments on photoproduction from deuterium in which only the charged pion was detected. The reactions studied were

$$\gamma + D \to \pi^+ + N + N \qquad (3a)$$

$$\gamma + D \to \pi^- + p + p \qquad (3b)$$

The DESY experiment covered photon energies of 3.4 to 5 GeV, and momentum transfers from near 0 to 0.6 GeV^2, while the SLAC experiment covered photon energies of 8 and 16 GeV and momentum transfers from 0 to roughly 1.5 GeV^2. These experiments, together with the earlier work of Bar-Yam et al.,[7] at CEA,

give π^- differential cross sections from deuterium which cover the entire range of energies over which π^+ production from the proton has been measured for momentum transfers $\lesssim 1.5$ GeV^2.

We are interested in obtaining from these data the cross section for π^- production from the free neutron. The cross section for π^- production from deuterium differs from that of the free neutron because of three effects--the Pauli exclusion principle, Glauber corrections, and other nuclear physics problems. The effect of the exclusion principle has been calculated by many authors[8] and is given by

$$\frac{d\sigma}{dt}(D\pi^-) = \left[1 - 1/3F(t)\right]\frac{d\sigma}{dt}(n\pi^-)_{\text{spin flip}} + \left[1 - F(t)\right]\frac{d\sigma}{dt}(n\pi^-)_{\substack{\text{non-spin}\\ \text{flip}}} \quad (4)$$

where F(t) is the deuteron form factor. Since the deuteron form factor falls very rapidly with momentum transfer, the Pauli principle correction also decreases rapidly with momentum transfer. The Glauber correction has been estimated to be of the order of 10% and the miscellaneous nuclear physics has been estimated to be of the order of 5 to 10%.[8] These effects are expected to be roughly the same for reactions (3a) and (3b).

Since the photoproduction cross section is a pure spin flip transition at zero degrees, if we assume that the relative amounts of spin flip and non-spin flip do not change wildly in the small momentum transfer region where the deuteron form factor is significant, the cross section for π^- production from the free neutron should be given to a good approximation by:

$$\frac{d\sigma}{dt}(n\pi^-) = \left[\frac{d\sigma}{dt}(D\pi^-)/\frac{d\sigma}{dt}(D\pi^+)\right]\frac{d\sigma}{dt}(p\pi^+) \equiv R\,\frac{d\sigma}{dt}(p\pi^+)\,. \quad (5)$$

The assumption made about the behavior of the relative amounts of spin flip and non-spin flip vs momentum transfer can itself be checked experimentally by studying the ratio of π^+ production from deuterium and π^+ production from hydrogen. Figure 4 summarizes all the data on this ratio. In general, the ratio of π^+ production from deuterium to the π^+ production from hydrogen behaves as we would expect the spin flip cross section to behave. Note that this ratio is not expected to go to one because of the Glauber correction and the other nuclear physics corrections.

With these preliminaries out of the way, we can now go on to the π^- production cross section from the neutron. Figure 5 shows all the data on the ratio of π^- production from deuterium to π^+ production from deuterium (R). The ratio R is about 1 in the forward direction, drops rapidly as $|t|$ increases, reaching 1/2 at $|t| \sim 0.1$ GeV^2, and reaching 0.3 at a $|t| \sim 0.3$ GeV^2. It then rises slowly as the momentum transfer increases. There appears to be a small systematic energy dependence of R--the high energy data tending to lie below the low energy data at small momentum transfers and above the low energy data at large momentum transfers.

Figure 6a shows the proton cross section measured from hydrogen and the neutron cross section as determined from Eq. (5). The neutron π^- cross section does not show the break slope at $|t| = m_\pi^2$ characteristic of π^+ data, but instead shows a smooth and very steep fall out to larger $|t|$. Figure 6b shows the cross section for the vector amplitude squared plus the scalar amplitude squared $\left[(1 + R)\frac{d\sigma}{dt}(p\pi^+)\right]$ and the cross section for the isovector-isoscalar interference $\left[(1 - R)\frac{d\sigma}{dt}(p\pi^+)\right]$. The square of the vector amplitude plus the square of the scalar amplitude shows the sharp forward spike and the interference cross section goes to zero in the forward direction.

The energy dependence of the data on R and 1 + R is shown in Figs. 7a and 7b. They were fit to

$$G(R) = f(t)\,(S - M^2)^{2\alpha}$$

$$\alpha_R = \alpha_N - \alpha_p \qquad (6)$$

$$\alpha_{1+R} = \alpha_{v^2+s^2} - \alpha_p \ .$$

The plots show both α_R and α_{1+R} to be near zero.

C. π^+ Production by Polarized Photons

The results of the first high energy experiment on π^+ photoproduction with polarized photons have been contributed to this Conference by a DESY group.[9] These experiments allow us to make further restrictions on the quantum numbers of the particles exchanged in the reaction. Only natural parity $\left[P = (-1)^J\right]$ exchange contributes to production when the γ-ray polarization is perpendicular to the production plane and only unnatural parity $\left[P = -(-1)^J\right]$ exchange contributes when the polarization is parallel to the production plane.

A polarized photon beam was produced by coherent bremsstrahlung from a diamond crystal. Figure 8 shows the energy spectrum and polarization of the beam. The peak in photon yield shown in Fig. 8 is due to coherent bremsstrahlung from the crystal lattice and the background is due to incoherent bremsstrahlung. Only the coherent bremsstrahlung is strongly polarized. The high energy edge of the coherent peak can be made extremely sharp by proper collimation of the incident electron beam. Both the height of the peak and its polarization increase when the energy of the peak is lowered with respect to the bremsstrahlung end point. The bremsstrahlung polarization vector is changed by rotation of the crystal about the incident beam direction.

The results of the DESY experiment are shown in Fig. 9. The difference over the sum of production perpendicular to and parallel to the production plane is plotted vs momentum transfer for various energies. The most extensive data have been obtained at 3.4 GeV. Since we have seen that the unpolarized differential cross section and the π^-/π^+ ratio in pion photoproduction have the same general character at 3.4 GeV as at 16 GeV, we may reasonably hope that these polarization results are characteristic of the high energy behavior of the cross section. The DESY results show that at $-t > m_\pi^2$ π^+ production goes almost entirely by natural parity exchange, i.e., π exchange contributes very little to the cross section. At $|t| = 0.06$ $\sigma_{\parallel}/\sigma_{\perp} \lesssim 5\%$ and at $|t| = 0.4$ $\sigma_{\parallel}/\sigma_{\perp} = 0.25$. This result is surprising to me and will place severe restrictions on models used to explain pion photoproduction. (Bar-Yam, Dowd, De Pagter, A. Kern have just reported a polarized photon measurement from the reaction $\gamma n \rightarrow \pi^- p$. They find $\Sigma = -0.08 \pm 0.2$ at $|t| = 0.6$ $(\text{GeV})^2$, and $\Sigma = +0.2 \pm 0.3$ at $|t| = 1.2$ $(\text{GeV})^2$.)

D. Comparison of the Data with Recent Theoretical Models.

There has been a great deal of work published in the last year interpreting charged pion photoproduction in terms of various forms of the Regge model. I want to compare three of the calculations, which represent what one might call different classes of the Regge model, with experiments. To be successful, a model must account for the π^+ differential cross section, the π^-/π^+ ratio from deuterium, and the cross section for production with polarized photons. The π^-/π^+ ratio from deuterium implies that at very small momentum transfers there can be only one G parity present in either the natural or unnatural spin parity sequence. The polarized photon data imply that at moderate momentum transfers the cross section is dominated by natural spin parity exchange and the π^-/π^+ ratio in this same region implies that both G parities are present.

The first model is that of the recent work by Brower and Dash.[10] This is the most ambitious attempt that I have seen to use only conspiring and nonconspiring Regge trajectories to fit the data. No cuts or fixed poles are allowed. The authors use a conspiring π trajectory and evasive ρ, A_2, and B trajectories. The model gives reasonable agreement with the π^+ differential cross section for momentum transfers to $|t| = 0.5$ GeV^2 and, if I put in the numbers correctly, is in qualitative agreement with the polarization data. This model, however, fails the test of the π^-/π^+ ratio for deuterium, giving a ratio considerably greater than that indicated by the data near $|t| = 0.5$. In addition, the energy dependence of the differential cross section will give increasing trouble beyond momentum transfers of 0.5 GeV^2.

The second model is that of Amati et al.[11] The authors use a phenomenological background containing both parities plus evasive π, B, and A_2 trajectories. The parameters of the background and the A_2 coupling were fit to the data and a quite good fit to the π^+ differential cross section was obtained as shown in Fig. 10. Unfortunately the model predicts a π^-/π^+ ratio >1 and is contradicted by the data. This is due to the sign chosen for the B coupling. At SLAC we have attempted to refit the data using the model of Amati et al., but with the opposite sign of the B coupling. However, we cannot get a decent fit to both the π^+ differential cross section and the π^-/π^+ ratio.

The third model is that of Frøyland and Gordon,[12] and this model uses π and ρ trajectories plus two cuts. The model agrees with the π^+ differential cross section out to momentum transfers of 2 GeV^2, with the π^-/π^+ ratio from deuterium, and with the polarization measured in the DESY experiment. Figure 11 shows the fit to the π^+ differential cross section. Figure 12 shows the π^-/π^+ ratio predicted, and Fig. 13 shows the polarization. The agreement is remarkable.

E. Vector Dominance and Charged Pion Photoproduction

In the vector dominance model the electromagnetic current is assumed to be identical to a linear superposition of vector-meson fields ($\rho\omega\phi$). The photon interacts with hadrons, as shown in the sketch below.

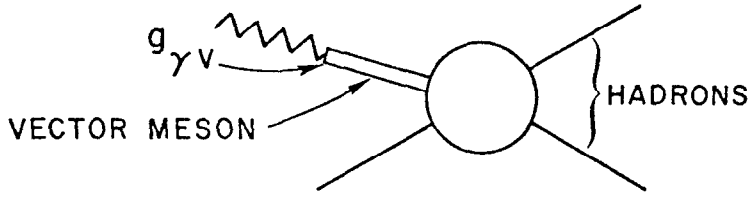

The photon turns into a vector meson with the appropriate coupling constant $g_{\gamma V}$ and then the vector meson interacts with hadrons. With this model and time reversal invariance it is possible to relate the amplitude for π-meson photoproduction to the amplitude for the production of transversely polarized vector mesons by pions as shown in Eq. (7):

$$A(\gamma N \longrightarrow \pi N') = \sum_{\rho\omega\phi} A(\pi N' \longrightarrow V_{tr} N) \tag{7}$$

We can square both sides of Eq. (7) and write a relation between cross sections as shown in Eq. (8):

$$\frac{d\sigma}{dt}(\gamma N \longrightarrow \pi N') = g^2_{\gamma\rho}\rho_{11}\frac{d\sigma}{dt}(\pi N' \longrightarrow \rho^o N) + g^2_{\omega\gamma}\rho_{11}\frac{d\sigma}{dt}(\pi N' \longrightarrow \omega^o N) + (\rho\omega \text{ interference}) + \tag{8}$$

where g^2 is the appropriate coupling constant which can be determined from other experiments, ρ_{11} is an element of the appropriate density matrix in the helicity frame and terms involving ϕ-mesons have been dropped, since these can be shown experimentally to be small. One must be cautious in dealing with the $\rho\omega$ interference terms —strictly speaking, they can only be handled if the details of the amplitudes are known. Relations between cross sections will be most reliable if the appropriate linear combination of cross sections is chosen in which the interference terms cancel.

Such a combination is

$$\frac{d\sigma}{dt}(\gamma p \to \pi^+ N) + \frac{d\sigma}{dt}(\gamma N \to \pi^- p) = 2g^2_{\gamma\rho}\rho_{11}\frac{d\sigma}{dt}(\pi^- p \to \rho^o N) + g^2_{\gamma\omega/}\rho_{11}\frac{d\sigma}{dt}(\pi^- p \to \omega^o N)$$

Recently Dar, Weisskopf, Levinson and Lipkin,[13] Diebold and Poirier,[14] Krammer and Schildknecht[15] have published comparisons of the π-meson photoproduction cross section with the predictions of the vector dominance model. Figure 14 shows a test of Eq. (9) from Dar et al., and Fig. 15 from Diebold and Poirier. Dar et al., and Krammer and Schildknecht used photon data from below 5 GeV and determined the elements of helicity density matrix by rotation of published data which were given in the Jackson frame. Diebold and Poirier used the 5 and 8-GeV photon data, and determined the helicity density matrix by refitting the raw data of Poirier et al.[16] The vector dominance model passes this test with flying colors.

Krammer and Schildknecht have also used a quark model relation to determine the difference between the cross sections for π^+ photoproduction from the proton and π^- photoproduction from the neutron, in terms of the cross section for $K^- p \to \bar{K}^{*o} n$ and $K^+ n \to K^{*o} p$. Figure 16 shows the results. The agreement is quite bad.

Dar and Weisskopf have predicted the ratio of π^-/π^+ photoproduction from deuterium by assuming a maximum interference between the ρ and ω amplitudes. Their results are shown in Fig. 17. In this case the agreement with the data is quite good.

Krammer and Schildknecht have also used the vector dominance model to predict the cross section for π photoproduction with polarized photons. Figure 18 shows the results, compared to the results of the DESY experiment. Again, the agreement is quite bad except at the $|t| < 0.1$ point in the 3.4 GeV data. This is not too surprising, since at all $|t| > 0.1$ (GeV)^2 the ρ-ω interference terms are important and the same quark model relation is involved in predicting this cross section as in

determining the difference between π^- and π^+ photoproduction cross sections. In view of the good agreement of the vector dominance model with ρ and ω data, the quark model relation should perhaps be re-examined.

II. π^o Photoproduction

A considerable amount of data on forward photoproduction of π^o mesons at energies up to 6 GeV has been obtained in the last three years by groups at DESY[17] and at CEA.[18] An experiment has recently been completed by the Ritson group at SLAC[19] which extends the energy range over which the π^o cross section has been measured up to 16 GeV. This experiment covers a range of momentum transfers from 0.2 to roughly 1.4 GeV^2. Only the lower energy experiments cover the region of very small momentum transfer.

The general characteristics of the data are a sharp spike in the cross section in the forward direction from π^o production in the Coulomb field of the nuclei (Primakoff effect), a moderately rapid fall with increasing momentum transfer out to a momentum transfer of about 0.5 GeV^2 (e^{5t}), a dip or break slope at $|t| = 0.5$, a relatively flat cross section out to a $|t|$ of 1.2, and again a falloff with increasing $|t|$. Data from CEA, DESY, and SLAC are shown in Fig. 19, where $(S - M^2)\frac{d\sigma}{dt}$ is plotted vs t. Only part of the existing data below 6 GeV are shown. Plotted in this way the data show almost no energy dependence except in the region of $|t| = 0.5$. There the SLAC data, which has the highest statistical accuracy in this region, show a small dip in the cross section at a photon energy of 6 GeV and no dip at all at a photon energy of 16 GeV.

The lowest mass particles which can be exchanged in the π^o photoproduction reaction are ρ and ω. If exchanged as elementary particles, without absorption, $d\sigma/dt$ at fixed momentum transfer should be independent of photon energy. Since the

data are clearly not independent of photon energy, the π^0 photoproduction reaction has been interpreted in terms of a model involving Reggeized ω and B-meson exchange. The ω exchange accounts for most of the cross sections, but ω exchange alone would give a zero in the cross section at $|t| = 0.5$, where the ω trajectory goes through 0. B-meson exchange fills in this dip. The specific model of Ader, Capdeville, and Salin[20] which has been used to fit the DESY data predicts that the dip in the cross section at $|t| = 0.5$ should become deeper as the energy increases, since the B trajectory lies below the ω trajectory.

The data of Fig. 19 near $|t| = 0.5$ show that the dip seems to be filling in as the energy increases. In addition, the energy dependence of the cross section outside the region of the dip seems incompatible with the simple picture of Reggeized ω exchange. Using a straight-line Regge trajectory, the 16 GeV data of the SLAC group should be a factor of about 2 above the 4-GeV data of DESY at $-t = 0.2$ and should be a factor of ~ 2 below the 4-GeV data at $-t = 0.8$. Since this is clearly not the case, we must conclude that this simple model does not work sufficiently well to account for the high energy data.

The Osborne group[21] at CEA has reported at this Conference on measurements of the cross section for $\gamma p \rightarrow \pi^0 p$ with polarized photons which also contradict the model using ω and B exchange. The polarized photon beam was produced by coherent bremsstrahlung from a crystal as described previously in the discussion of the DESY experiment on π^+ production with polarized photons. The results of this experiment are shown in Fig. 20 where $(\sigma_\perp - \sigma_\parallel) / (\sigma_\perp + \sigma_\parallel)$ is plotted vs t. The results show that at the point where the ω trajectory goes through zero $R \approx 0.5$ which implies that $\sigma_\perp / \sigma_\parallel \approx 3$, i.e., the cross section is dominated by natural spin-parity exchange.

Harari[22] has assumed the validity of the vector dominance model and uses this assumption to test the hypothesis that π^0 photoproduction goes through

Reggeized ω and B exchange. In this model, at the point where the ω trajectory passes through 0, the π^0 photoproduction proceeds via isoscalar photons, and the π^0 cross section is given in the vector dominance model by

$$\frac{d\sigma}{dt}(\gamma p \to \pi^0 p) = \frac{g^2_{\omega\gamma}}{4} \frac{d\sigma}{dt}(\pi^- p \to \omega_{tr} N). \tag{10}$$

Harari finds that the π-ω cross section is too small by a factor of 10 to account for π^0 photoproduction at this momentum transfer. By pushing all errors to their limits, he can reduce the discrepancy to a factor of 4. Since the π-ω cross section determines the sum of <u>all</u> isovector exchanges, the Regge model is in serious difficulty.

The implications of the π^0 photoproduction experiments for the Regge theory can be summarized as follows. In the region of the "dip,"

1) isoscalar exchange is required (Harari-vector dominance)
2) natural spin-parity exchange is required (Osborne-polarized photon experiments)
3) $\alpha(t) \geq 0$ for $|t| \lesssim 1$ GeV^2 (Ritson - π^0 cross section measurements)
4) charge conjugation = (-1) (conservation of c)

There is no established or conjectured particle in the latest edition of the Rosenfeld table that fulfills requirements 1, 2, and 4 except the ϕ and the ω (the ϕ is usually ignored in these discussions, but since we are grasping at straws, we will keep it). Either the ω and or ϕ have very strange trajectories, or something equivalent to poles or cuts is required; or the Regge model must be abandoned. I am sure the theorists will find a way around this problem with dispatch.

Dar, Weisskopf, Levinson, Levinson and Lipkin[13] have compared the vector dominance prediction of π^o photoproduction with the experimental data. They write the π^o cross section as

$$\frac{d\sigma}{dt}\left(\gamma_N^P \to \pi^o{}_N^P\right) = \frac{1}{2}\left\{g_{\rho\gamma}\left[\frac{d\sigma}{dt}\left(\pi^o p \to \rho_{tr} p\right)\right]^{1/2} \pm g_{\omega\gamma}\left[\frac{d\sigma}{dt}\left(\pi^o p \to \omega_{tr} p\right)\right]^{1/2}\right\}^2$$

where the + and - signs on the right-hand side of Eq. (1) refer to π^o photoproduction from the proton and neutron, respectively, ρ_{tr} and ω_{tr} indicate the cross section for production of ρ and ω mesons transversely polarized in the helicity frame, and the relative phase of the ρ and ω contributions comes from SU6. The cross sections on the right-hand side of Eq. (1) are of course unmeasurable, but they can be obtained by using isospin relations from measurable quantities as follows:

$$\frac{d\sigma}{dt}\left(\pi^o p \to \rho^o p\right) = \frac{1}{2}\left[\frac{d\sigma}{dt}(\pi^- p \to \rho^- p) + \frac{d\sigma}{dt}\left(\pi^+ p \to \rho^+ p\right) - \frac{d\sigma}{dt}(\pi^- p \to \rho^o N)\right] \tag{12}$$

$$\frac{d\sigma}{dt}(\pi_0 p \to \omega^o p) = \frac{1}{2}\frac{d\sigma}{dt}(\pi^- p \to \omega n). \tag{13}$$

The results of applying these relations are shown in Fig. 21. In Fig. 21a, the curve labeled ρ gives the square of the amplitude for all isoscalar exchanges and the curve labeled ω gives the square of the amplitude for all isovector exchanges. The curves are fitted to the data by eye and the ρ curve is very badly determined in the region $0.2 < -t < 0.6$. Figure 21b shows the comparison to the π^o photoproduction data. The theoretical curve agrees fairly well with the data, but in view of the large uncertainty in the $\pi\rho$ data near the dip in the π^o cross section, agreement between the curve and experiment in this region should be regarded as fortuitous.

A report on a new measurement of the π^o lifetime has been contributed to this Conference by the group of Braunschweig, Braunschweig, Husmann, Lübelsmeyer,

and Schmitz working at DESY.[17] They have measured the π^o photoproduction cross section in Coulomb field of a proton. Their data are shown in Fig. 22. The sharp rise in the cross section at 0^o is presumably due to the Primakoff effect. The curves show a fit to the data using the Primakoff effect plus Reggeized ω exchange, the solid curves being for constructive interference and the dashed for destructive interference. The π^o lifetime obtained is strongly sensitive only to the assumption that the background under the Primakoff peak goes to 0 at 0^o and is not too sensitive to the detailed shape of the background. The value of the π^o lifetime obtained is

$$\tau_{\pi^o} = \left(0.6^{+0.2}_{-0.08}\right)\times 10^{-16} \text{ sec}, \tag{14}$$

which gives

$$\Gamma(\pi^o \longrightarrow \gamma\gamma) = 11^{+1.6}_{-2.8} \text{ volts}. \tag{15}$$

This new lifetime still does not remove the discrepancy between the SU3 prediction <u>without</u> $\eta - X^o$ mixing of the ratio of the partial width of $\pi^o \rightarrow 2\gamma$ and $\eta \rightarrow 2\gamma$. Using the measurements of Bemporad <u>et al.</u>[23] on the Primakoff effect in η production from complex nuclei and the measurements of Baltay <u>et al.</u>[24] on the branching ratio of $\eta \rightarrow 2\gamma$, we find

$$\Gamma(\eta \rightarrow \gamma\gamma) \approx 1 \pm 0.15 \text{ keV}. \tag{16}$$

The SU3 prediction is

$$\left[\frac{\Gamma(\eta \rightarrow \gamma\gamma)}{\Gamma(\pi^o \rightarrow \gamma\gamma)}\right]_{SU3} \times \Gamma(\pi^o)_{exp} = 235^{+35}_{-60} \text{ eV}. \tag{17}$$

III. Photoproduction of N* (1238)

My group at SLAC has reported at this Conference[25] on the results of cross section measurements of the reaction

$$\gamma + p \longrightarrow \pi^- + N^{*++}(1238). \tag{18}$$

The experiment was done by detecting only the π^- and fitting the excitation function with the N* and various combinations of background terms. The results are shown in Fig. 23, where the errors on the points include our estimate of the variation of the cross section with different background models. The dashed lines on the graph are the differential cross sections for the reaction $\gamma p \rightarrow \pi^+ n$. The results of this experiment are somewhat surprising. At momentum transfers ≥ 0.2 GeV^2 the N* cross section is quite close to the cross section for single π^+ production. As the momentum transfer decreases the differential cross section rises sharply $\left(\frac{d\sigma}{dt} \approx e^{12t}\right)$, reaching a maximum of roughly six times the π^+ cross section at small momentum transfer. The N* cross section then dips down as the momentum transfer goes toward the minimum momentum transfer. The small momentum transfer data are shown on an expanded scale in Fig. 24, where $(S - M^2)^2 \frac{d\sigma}{dt}$ is plotted vs $\sqrt{|t|}$. Plotted in this way, the data seem to be independent of photon energy. The dip in the forward differential cross section is clear but it is not clear whether the cross section extrapolates to zero or a finite value of $|t| = 0$. We do not think that these data can be much improved, since uncertainties in the background subtraction under the N* contribute an error comparable to the statistical error at the small momentum transfer points. Figure 25 shows the parameter α of Eq. (1) for the N* reaction. α remains near 0 for the entire range of momentum transfers covered. We have seen in the case of $\gamma p \longrightarrow \pi^+ N$ and $\gamma p \longrightarrow \pi^- N$ that the $(S - M^2)^2\, d\sigma/dt$

is nearly independent of energy over the range of roughly 2 - 16 GeV. It should then be no surprise that the same thing seems to happen in $\gamma p \rightarrow \pi^- N^{*++}$. When scaled in this way, the DESY bubble chamber[26] data are consistent for $|t|<0.3$ with the SLAC data for all energies above 1.4 GeV. At $|t|>0.3$ there is insufficient bubble chamber data to allow a comparison.

The N* photoproduction data can be compared to the cross sections for $\pi^+ p \rightarrow \rho^o N^{*++}$ and $\omega^o N^{*++}$ using the vector dominance model and S - U crossing. Dar and Weisskopf and Iso and Yoshii[27] have made such comparisons using the DESY bubble chamber data for the γ cross sections, and data from several bubble chamber experiments for the π cross sections. I have added points from the high energy photoproduction experiment to the Dar and Weisskopf graph, and the results are shown in Fig. 26. The shape is approximately correct, but the normalization is off. The principal contributors of the bubble chamber data, the ABC collaboration (private communication from D. R. O. Morrison) have urged great caution in using the $N^{*++}\rho^o$ cross section since they consider that there is no satisfactory method for determining this cross section. With this in mind we can only conclude that the agreement may be better or worse than indicated in Fig. 26, but that whatever causes the steep rise for $|t|<0.2$ $(GeV)^2$ in the photoproduction reaction, also causes such a rise in the $N^*\rho$ reaction.

IV. Charged K-meson Photoproduction

The only new data on charged K-meson photoproduction come from my group at SLAC[28] where we have extended our measurement on the reactions

$$\gamma + p \rightarrow K^+ + \Lambda^o \qquad (19a)$$

$$\gamma + p \rightarrow K^+ + \Sigma^o \quad . \qquad (19b)$$

The statistics at small momentum transfers have been improved, and the measurements extended to cover larger momentum transfers. The differential cross section for the reaction $\gamma + p \rightarrow K^+ + \Lambda^o$ is shown in Fig. 27. The data show a sharp dip at small momentum transfer in contrast to the π^+ data which show a sharp rise. At large momentum transfer the data show that the same slope as is shown in π^+ production and the K - Λ differential cross section is about 1/3 of the π^+ differential cross section. The energy dependence of the cross section at fixed momentum transfer was determined by fitting the data to the form of Eq. (1). The parameter α is plotted vs t in Fig. 28. The figure shows that α is quite small to momentum transfers of -2 GeV^2. Figure 29 shows the ratio of $K^+\Sigma^o/K^+\Lambda^o$ production as a function of momentum transfer. This ratio is consistent with 1 at all photon energies except in the region of very small momentum transfers. The low energy data show the Σ/Λ ratio decreasing as $-t \rightarrow 0$. The higher energy data do not show this trend but they do not go down to as small a momentum transfer.

The π, KΛ, and KΣ data can be used to test the SU3 prediction of the following relations between the amplitudes for these three processes:

$$\sqrt{2}\ A(\pi^+N) = -\sqrt{3}\ A(K^+\Lambda^o) - A(K^+\Sigma^o). \tag{20}$$

This relation between amplitudes can be turned into relation between cross sections as follows:

$$2\sigma(\pi N) = \left|\left[3\sigma(K\Lambda)\right]^{\frac{1}{2}} + \left[\sigma(K\Sigma)\right]^{\frac{1}{2}} \cdot e^{i\phi}\right|^2 \tag{21}$$

where ϕ is the relative phases of the amplitudes. We have used the new SLAC data to test these relations. In Fig. 30 $\cos\phi$ is plotted vs momentum transfer for energies from 5 to 16 GeV. The SU3 relation is good if $\cos\phi$ lies between ± 1. The data show

that SU3 is indeed satisfied for all momentum transfers >0.1 GeV^2 but is badly broken for momentum transfers smaller than this value. This is a consequence of the sharp rise in the π^+ cross section and the sharp fall in the K cross section at small momentum transfers.

There has not been a great deal of theoretical activity on K photoproduction in the past year. Two sets of authors—Ball, Frazer and Jacob[29] and Henyey[30]—have tried to analyze both the forward π photoproduction and K photoproduction data in terms of a Regge conspiracy model and both have reached what I would call qualitatively similar conclusions. Ball, Frazer and Jacob find that the very forward momentum transfer K data are consistent with a conspiracy model, although with a weaker conspiracy than occurs in the case of the pion. Henyey finds that the small momentum transfer K data are consistent with no conspiracy at all. Both find that, except at the very most forward points, K exchange must in fact contribute little to the cross section and the cross section must be dominated by something like K* exchange. The reason for this conclusion is that, using the $K\Lambda$ and $K\Sigma$ coupling constants derived recently by Kim,[31] one should find very small Σ production relative to Λ production. Since the data indicate comparable Λ and Σ production, K exchange must be excluded as the dominant mechanism in Λ and Σ photoproduction.

Meshkov and Ponzini[32] have used SU6(W) to predict the ratio of forward $K\Lambda/K\Sigma$ photoproduction. They find that this ratio should be between 0.5 and 1 in a photon energy range of 5 to 16 GeV, which is in quite good agreement with the data and represents an improvement over the prediction of Lipkin and Scheck[33] based on the quark model that these cross sections should be in a ratio of 1/27. However, SU6(W) is based on SU3 and we have seen that SU3 is violated at small momentum transfer based on the breakdown of the triangle inequality of Eq. (21). Meskov and Ponzini blame the SU3 violation on the π, and assume that SU3 and hence SU6(W) is good for predicting relative $K\Lambda$ and $K\Sigma$ cross sections.

V. Miscellaneous

Diebold[34] at SLAC has been making a compilation of integrated cross sections as a function of energy for various photoproduction reactions. At low energies complete angular distributions are available and the integration is easy. At high energies the forward cross section is known and some measurements have been made in the backward direction. These backward cross sections give limits on the intermediate $|t|$ region, and Diebold estimates that the integrated cross sections should be accurate to 5 - 10%. Figures 31 and 32 show $k^2 \sigma_{Total}\left(k^2 \propto (S - M^2)^2\right)$ vs k for various reactions. All of these reactions show an astonishing similarity - $k^2\sigma_T$ tends to become constant at an energy between 1.5 and 4 GeV.

VI. Summary and Conclusions

Recent photoproduction experiments at CEA, DESY and SLAC have given a wealth of information on the photoproduction of pseudoscalar mesons. We now have available differential cross sections for production from the proton and the neutron with polarized and unpolarized photon beams. These experiments impose several restrictions on theoretical models and will hopefully clear up some of the existing theoretical ambiguities. I would summarize what we have learned from photoproduction studies in the past year as follows.

1. The vector dominance model works well when combinations of cross sections can be used in which $\rho - \omega$ interference terms cancel out. When the ρ-ω interference term is important, reasonable assumptions on the relative phase of the ρ and ω amplitudes yield good agreement between reactions involving photons and reactions involving vector mesons.

2. The photon is not a special object which gives rise to features in various cross sections which are not seen in hadron induced reactions. This is of course implied by the success of vector dominance. However the photon could be special if the vector mesons were also.

3. Charged pion photoproduction implies that theories using only linear Regge trajectories are untenable and that theories using linear conspiring trajectories will probably not work.

4. π^o photoproduction leads to stronger conclusions. Linear trajectories will not work.

5. The N* production cross section measurements have shown some peculiar features which need to be explained. Among these are the rough equality with π^+ cross sections seen at $|t| > 0.2$ $(\text{GeV})^2$, the e^{12t} behavior seen for $m_\pi^2 < |t| < 0.2$, and the decrease in the cross section for $|t| < m^2$.

6. SU3 fails to properly predict the relation between the cross section for production of members of the pseudoscalar octet. However the failure occurs in a region of t where mass difference effects may be important.

7. All the well measured pseudoscalar meson production cross sections exhibit a k^{-2} behavior. The differential cross sections also exhibit roughly the same k^{-2} dependence out to $|t| > 1$ $(\text{GeV})^2$ with the exception of a limited t region near $|t| = 0.5$ in π^o production. This regularity seems to begin at photon energies of around 2 GeV.

There are still other features of the data which might be mentioned, but I think there are sufficient to generate a great deal of thought. Hopefully, they will all be explained by the next conference.

REFERENCES

1. A. M. Boyarski, F. Bulos, W. Busza, R. Diebold, S. D. Ecklund, G. E. Fischer, Y. Murata, B. Richter, and W. S. C. Williams, Conference contribution (1968).
2. A. M. Boyarski, F. Bulos, W. Busza, R. Diebold, S. D. Ecklund, G. E. Fischer, J. Rees, B. Richter, Phys. Rev. Letters 20, 300 (1968).
3. G. Buschhorn, J. Carroll, R. D. Eandi, P. Heide, R. Hübner, W. Kern, U. Kötz, P. Schmüser, H. J. Skronn, Phys. Rev. Letters 17, 1027 (1966); Phys. Rev. Letters 18, 511 (1967).
4. See, for example, S. D. Drell and J. D. Sullivan, Phys. Rev. Letters 19, 268 (1967).
5. P. Heide, U. Kötz, R. A. Lewis, P. Schmüser, H. J. Skronn, H. Wahl, Phys. Rev. Letters 21, 248 (1968).
6. A. M. Boyarski, R. Diebold, S. D. Ecklund, G. E. Fischer, Y. Murata, B. Richter, and W. S. C. Williams, Conference contribution (1968).
7. Z. Bar-Yam, J. De Pagter, M. M. Höenig, W. Kern, D. Luckey, and L. S. Osborne, Phys. Rev. Letters 19, 40 (1967).
8. A. Dar and A. Gal, M. I. T. Preprint CTP 28 (1968) and K. Schilling, DESY Preprint 68/35 (1968).
9. Chr. Geweniger, P. Heide, U. Kötz, R. A. Lewis, P. Schmüser, H. J. Skronn, H. Wahl, K. Wegener, Conference contribution (1968).
10. R. Brower and J. W. Dash, UCRL 18199 (1968).
11. D. Amati, G. Cohen-Tannoudji, R. Jengo, and Ph. Salin, Phys. Letters 26B, 510 (1968).
12. J. Frøyland and D. Gordon, M. I. T. Preprint CTP 38 (1968).
13. A. Dar, V. F. Weisskopf, C. A. Levinson, and H. J. Lipkin, Phys. Rev. Letters 20, 1261 (1968).

14. R. Diebold and J. A. Poirier, Phys. Rev. Letters 20, 1532 (1968).

15. M. Krammer and D. Schildknecht, DESY Report 68/33 (1968).

16. Notre Dame-Purdue-SLAC-LRL collaboration, to be published in Phys. Rev.

17. M. Braunschweig, W. Braunschweig, D. Husmann, K. Lübelsmeyer, D. Schmitz, Phys. Letters 26B, 405 (1968) and Conference contribution.

18. G. C. Bolon, D. Garelick, S. Homma, R. Lewis, W. Lobar, D. Luckey, L. S. Osborne, R. Schwitters, J. Uglum, Phys. Rev. Letters 18, 926 (1967).

19. R. Anderson, D. Gustavson, J. Johnson, D. Ritson, W. G. Jones, D. Kreinick, F. Murphy, R. Weinstein, Phys. Rev. Letters 21, 384 (1968) and Conference contribution.

20. J. P. Ader, M. Capdeville, Ph. Salin, Nucl. Phys. 33, 407 (1967).

21. D. Bellenger, R. Bordelon, K. Cohen, S. Deutsch, W. Lobar, D. Luckey, L. S. Osborne, E. Pothier, and R. Schwitters, Conference contribution.

22. H. Harari, SLAC Preprint PUB-477 (1968).

23. C. Bemporad, P. Braccini, L. Foa, K. Lübelsmeyer, and D. Schmitz, Phys. Letters 25B, 380 (1967).

24. C. Baltay, P. Franzini, J. Kim, L. Kirsch, R. Newman, N. Yeh, J. Cole, J. Lee-Franzini, and H. Yarger, Phys. Rev. Letters 19, 1498 (1967).

25. A. M. Boyarski, R. Diebold, S. D. Ecklund, G. E. Fischer, Y. Murata, B. Richter, and W. S. C. Williams, Conference contribution (1968).

26. ABB HHM collaboration DESY report 68/8 (1968).

27. Dar and Weisskopf CERN Preprint 68/9M/5 (1966). Iso and Yoshii, Ann. Phys. (1966).

28. A. M. Boyarski, F. Bulos, W. Busza, R. Diebold, S. D. Ecklund, G. E Fischer, Y. Murata, B. Richter, and W. S. C. Williams, Conference contribution (1968).

29. J. Ball, W. Frazer, and M. Jacob, Phys. Rev. Letters 20, 518 (1968).

30. F. Henyey, Phys. Rev. 170, 1619 (1968).

31. J. K. Kim, Phys. Rev. Letters 19, 1074 (1967).

32. S. Meshkov and R. Ponzini, NBS Preprint (1968).

33. H. J. Lipkin and F. Scheck, Phys. Rev. Letters 18, 347 (1967).

34. R. Diebold, private communication.

FIGURE CAPTIONS

1. π^+ Photoproduction Cross Section Plotted vs Momentum Transfer. The data are from Refs. 1-3.
2. Small Momentum Transfer π^+ Photoproduction Data Plotted on an Expanded Scale. The data are from Refs. 1 and 2.
3. Energy Dependence of the π^+ Photoproduction Data. $\alpha(t)$ is defined in Eq. (1).
4. Ratio of π^+ Photoproduction Cross Section from Deuterium to the π^+ Photoproduction Cross Section from Hydrogen. Data are from Refs. 5-7.
5. Ratio of π^- Photoproduction Cross Section from Deuterium to the π^+ Photoproduction Cross Section from Deuterium. Data are from Refs. 5-7.

6a. The Cross Section for π^+ Production from the Proton and π^- Production from the Neutron at 8 and 16 GeV. Data are from Ref. 6.

6b. Differential Cross Sections for the Sum and Difference of π^+ Production from the Proton and π^- Production from the Neutron.

7a. Energy Dependence of the π^-/π^+ Cross Section Ratio. $\alpha(R)$ is defined in Eq. (6).

7b. Energy Depencence of the Sum of π^+ and π^- Cross Sections. α is defined in Eq. (6).

8. Proton Energy Spectra and Polarization for the DESY Polarized Photon Beam from Ref. 9.
9. The Difference over the Sum of Cross Sections for Photoproduction with the Polarization Perpendicular to and Parallel to the Production Plane from Ref. 9.
10. The Fit of Amati et al., to the π^+ Photoproduction Data.
11. The Fit of Frøyland and Gordon to the π^+ Photoproduction Data.
12. The π^-/π^+ Ratio in the Model of Frøyland and Gordon.
13. The prediction of Frøyland and Gordon for π^+ Photoproduction by Polarized Photons.
14. Comparison of Ref. 13, using the Vector Dominance Model, of ρ and ω Production by Pions to π^+ Photoproduction.

15. Comparison of Ref. 14, using the Vector Dominance Model, of ρ and ω Production by Pions to π^+ Photoproduction.

16. Comparison of Ref. 15, using the Vector Dominance and Quark Models, of the Production of K*'s and K's to the Difference between π^+ Production from the Proton and π^- Production from the Neutron.

17. Comparison of Ref. 13, using the Vector Dominance Model, of ρ and ω Production by Pions to the Ratio of π^-/π^+ Photoproduction from Deuterium.

18. Vector Dominance and Quark Model Prediction of the Cross Section for π^+ Photoproduction by Polarized Photons from Ref. 15.

19. π^o Photoproduction Cross Sections from Refs. 17-19.

20. π^o Photoproduction Cross Sections with Polarized Photons from Ref. 20.

21. Vector Dominance Prediction of the π^o Photoproduction Cross Section from Ref. 13.

22. Forward π^o Photoproduction Cross Section from Ref. 17.

23. Cross Section for Photoproduction for $\pi^- N^{*++}$ (1238) from Ref. 24.

24. N^* Photoproduction Cross Section at Small Momentum Transfers on an Expanded Scale.

25. Energy Dependence of the N^* Photoproduction Cross Section at Fixed Momentum Transfer.

26. Vector Dominance Comparison of $\gamma p \rightarrow \pi N^*$ and $\pi^+ p \rightarrow \rho^o N^*$ and $\omega^o N^*$ from Ref. 24b.

27. Differential Cross Section for the Photoproduction of $K^+\Lambda^o$ from Ref. 26.

28. Energy Dependence of the $K^+\Lambda^o$ Photoproduction Cross Section from Ref. 26.

29. Ratio of $K^+\Sigma^o/K^+\Lambda^o$ Photoproduction Cross Section from Ref. 26.

30. Test of the SU3 Triangle Inequality using the Data of Ref. 26.

31. Total Cross Section for Various π Photoproduction Reaction vs Photon Energy from Ref. 34.

32. Total Cross Section for Various K Photoproduction Reactions vs Photon Energy from Ref. 34.

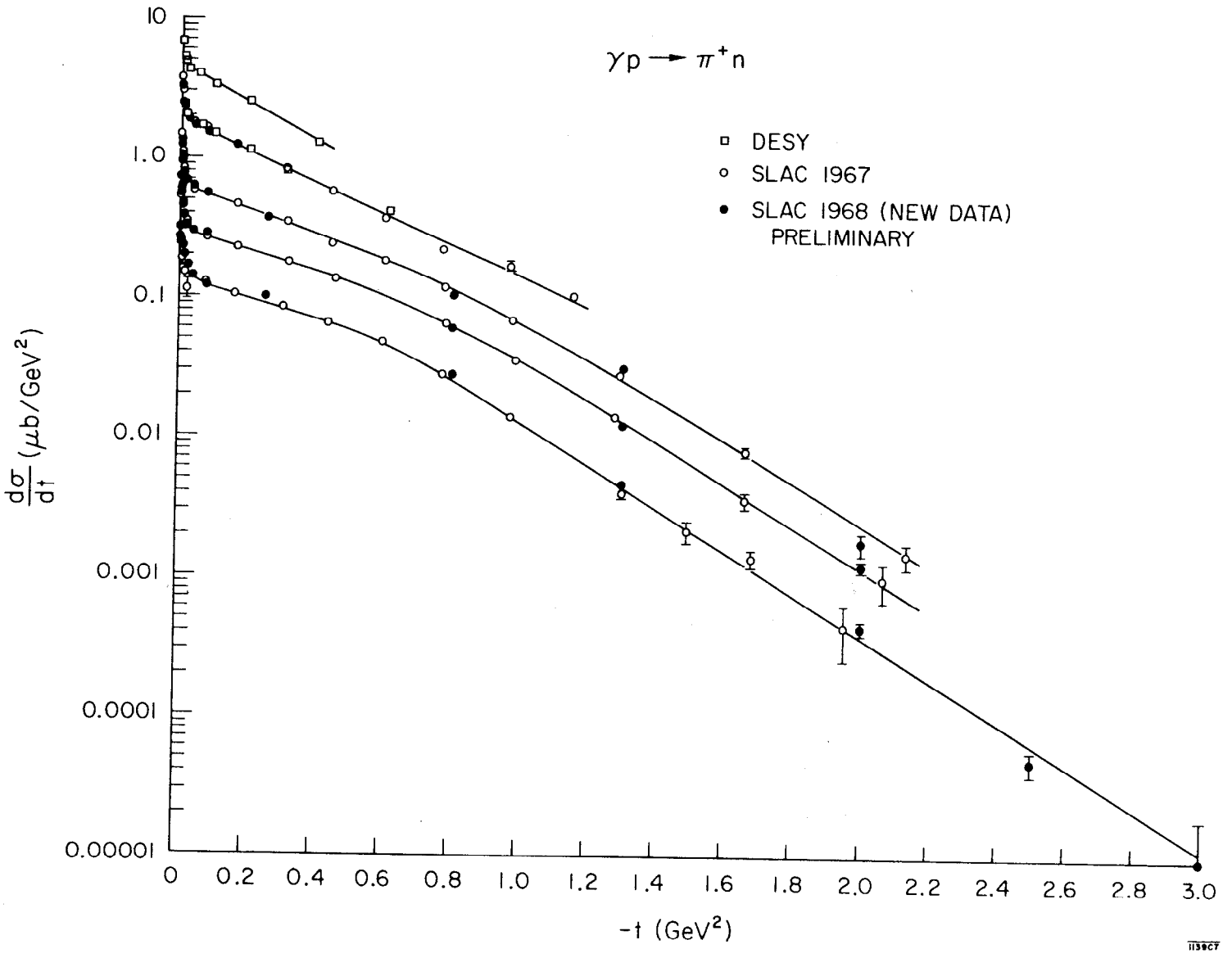
$\gamma p \rightarrow \pi^+ n$
DESY
SLAC 1967
SLAC 1968 (NEW DATA)
PRELIMINARY
$\frac{d\sigma}{dt}$ (μb/GeV^2)
10
1.0
0.1
0.01
0.001
0.0001
0.00001
0
0.2
0.4
0.6
0.8
1.0
1.2
1.4
1.6
1.8
2.0
2.2
2.4
2.6
2.8
3.0
-t (GeV^2)
1135C7

Fig. 1

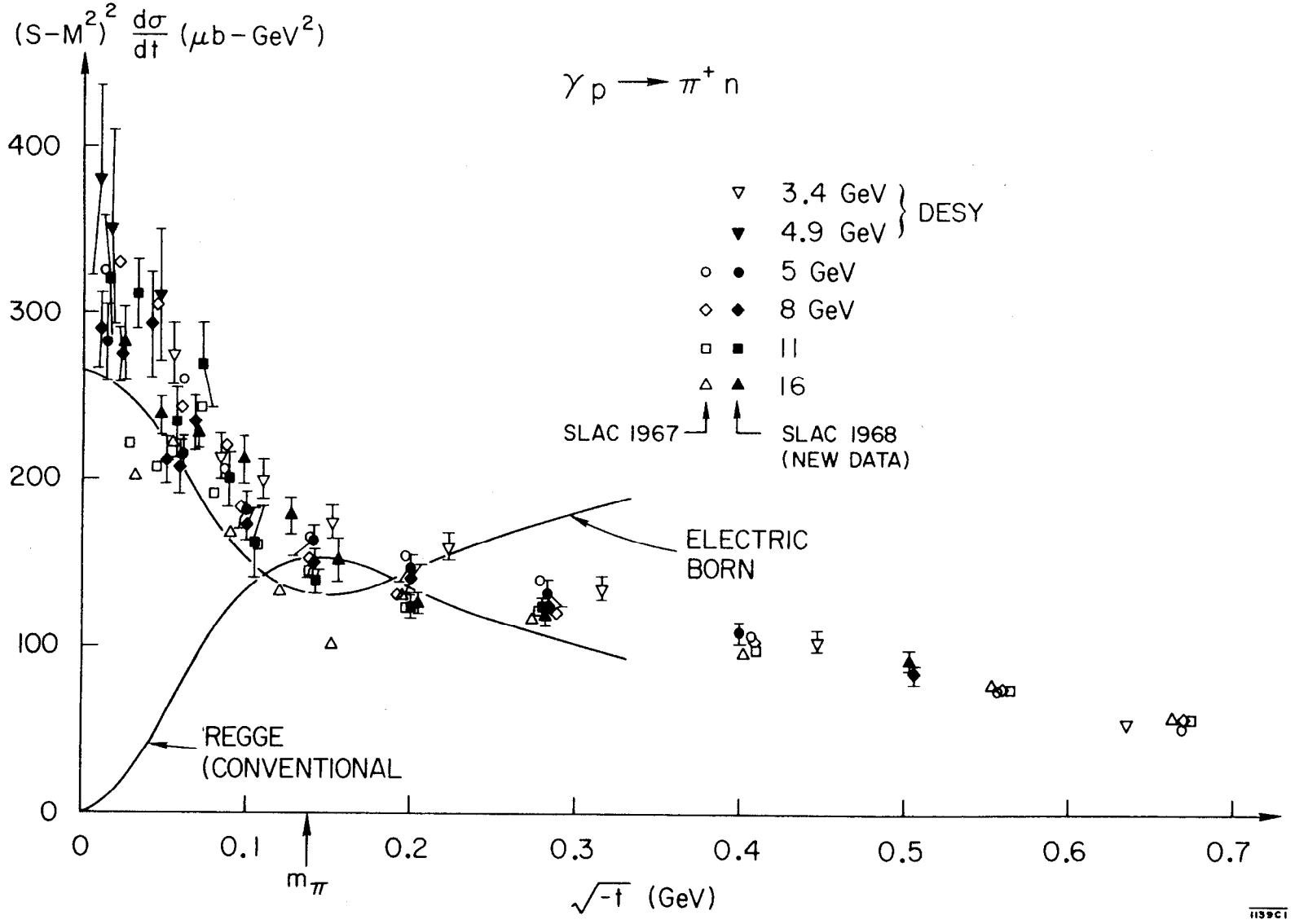
$(S-M^2)^2 \frac{d\sigma}{dt}$ (μb − GeV^2)
$\gamma p \rightarrow \pi^+ n$
400
300
200
100
0
3.4 GeV
4.9 GeV
DESY
5 GeV
8 GeV
11
16
SLAC 1967
SLAC 1968
(NEW DATA)
ELECTRIC
BORN
REGGE
(CONVENTIONAL
0
0.1
0.2
0.3
0.4
0.5
0.6
0.7
m_π
$\sqrt{-t}$ (GeV)
1139C1

Fig. 2

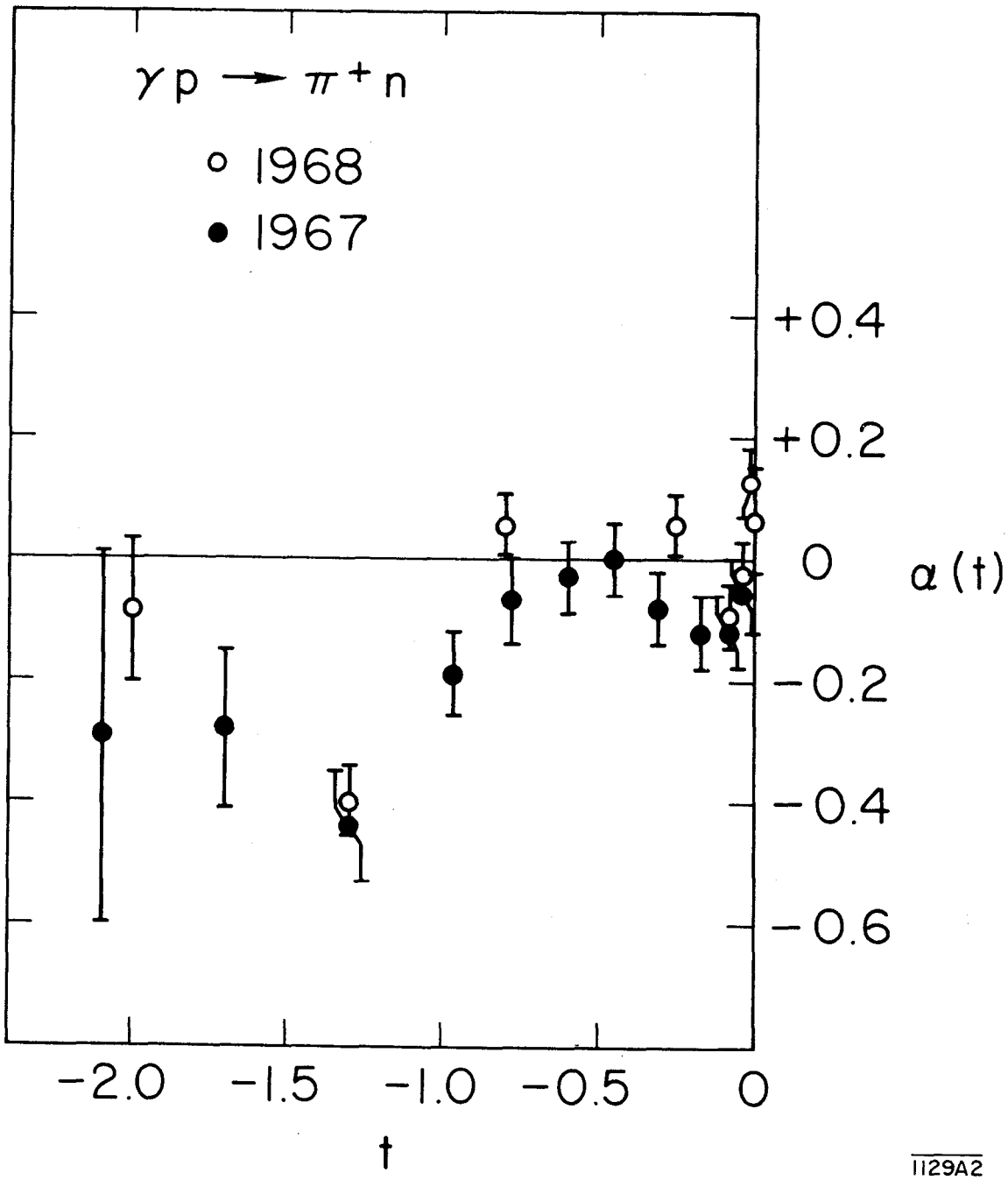

Fig. 3

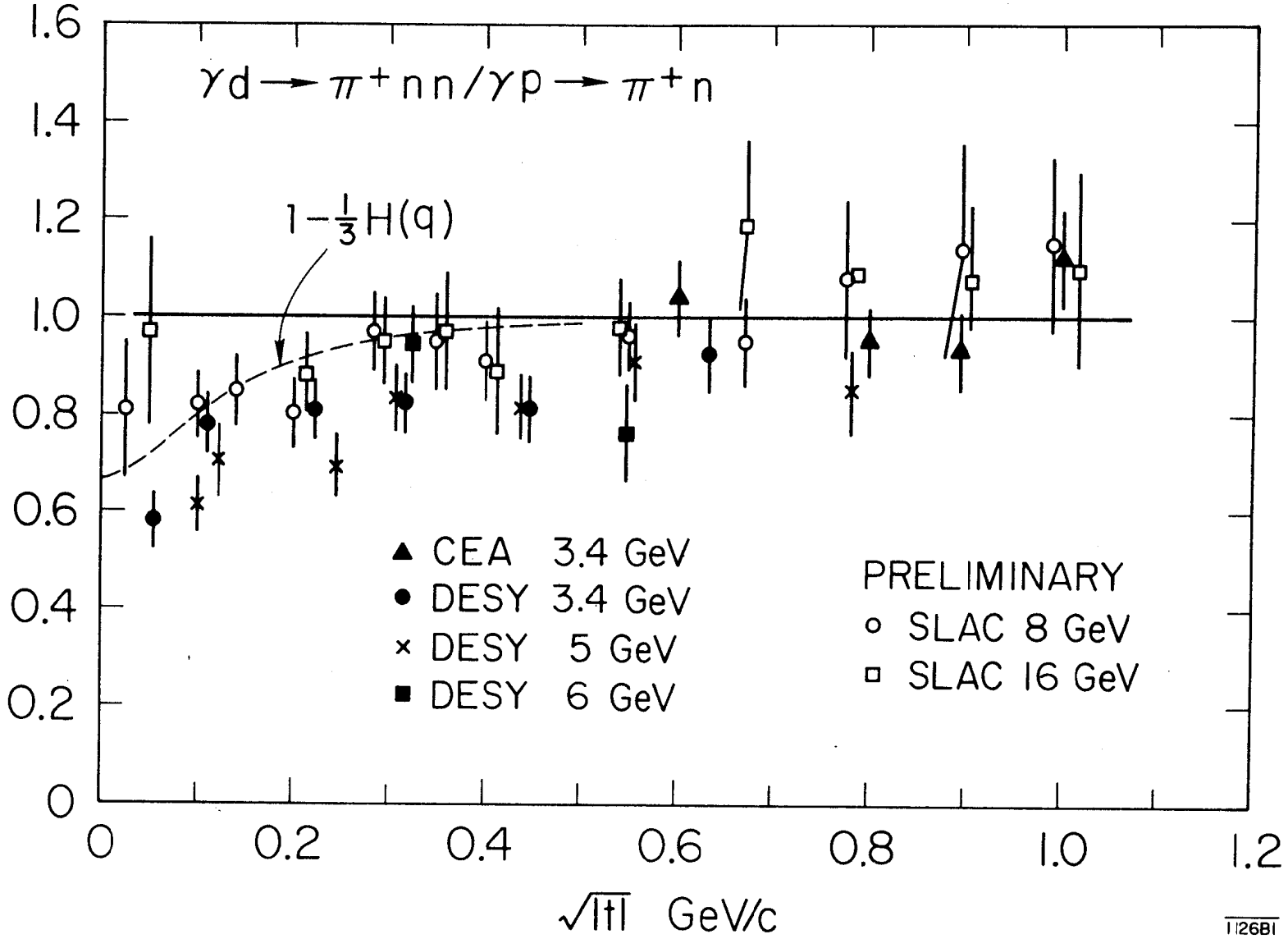
$\gamma d \rightarrow \pi^+ nn / \gamma p \rightarrow \pi^+ n$
$1-\frac{1}{3}H(q)$
▲ CEA 3.4 GeV
● DESY 3.4 GeV
× DESY 5 GeV
■ DESY 6 GeV
PRELIMINARY
○ SLAC 8 GeV
□ SLAC 16 GeV
1.6
1.4
1.2
1.0
0.8
0.6
0.4
0.2
0
0
0.2
0.4
0.6
0.8
1.0
1.2
$\sqrt{|t|}$ GeV/c
1126B1

Fig. 4

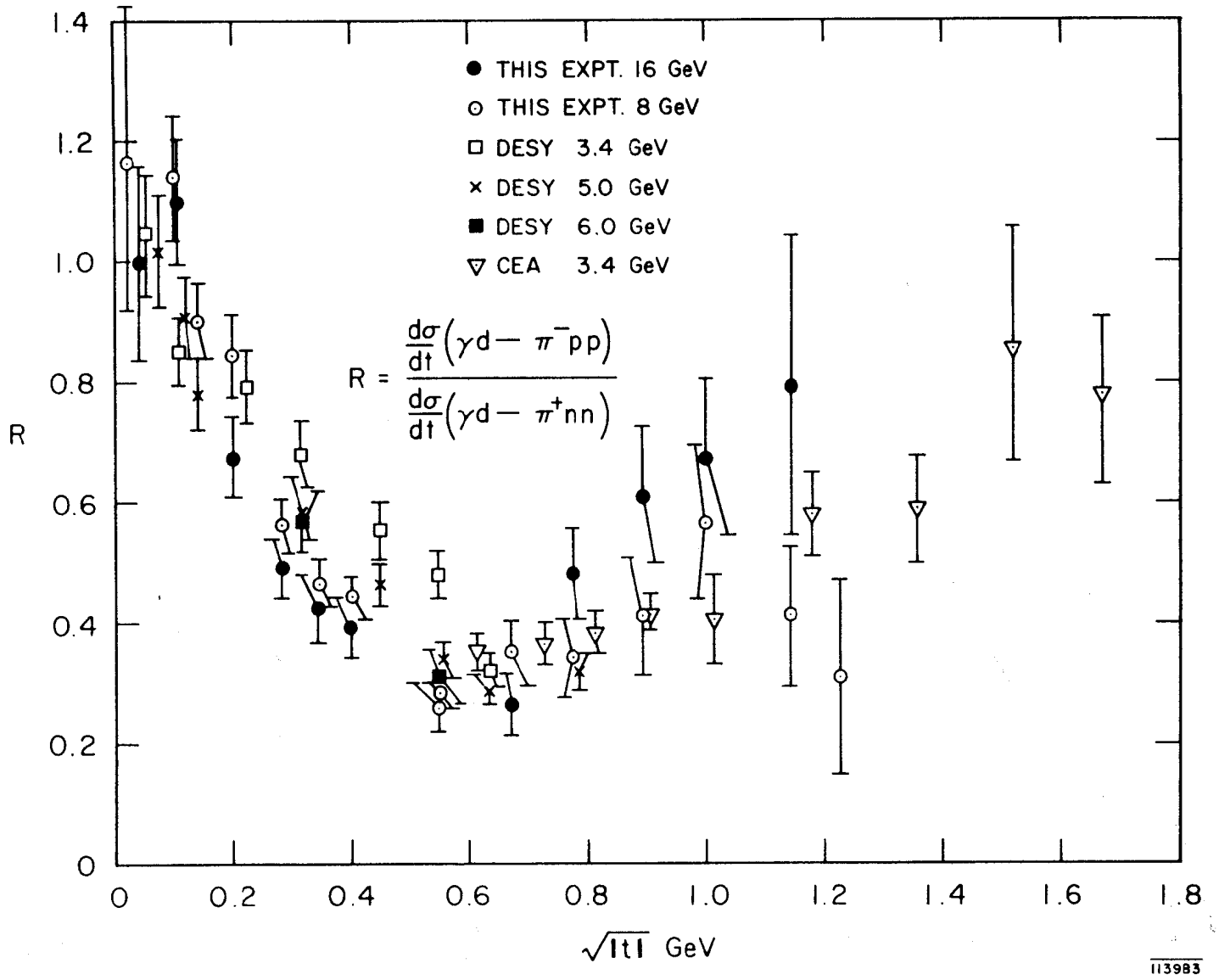
THIS EXPT. 16 GeV
THIS EXPT. 8 GeV
DESY 3.4 GeV
DESY 5.0 GeV
DESY 6.0 GeV
CEA 3.4 GeV
$R = \frac{\frac{d\sigma}{dt}(\gamma d - \pi^- pp)}{\frac{d\sigma}{dt}(\gamma d - \pi^+ nn)}$
R
$\sqrt{|t|}$ GeV
0
0.2
0.4
0.6
0.8
1.0
1.2
1.4
1.6
1.8
113983

Fig. 5

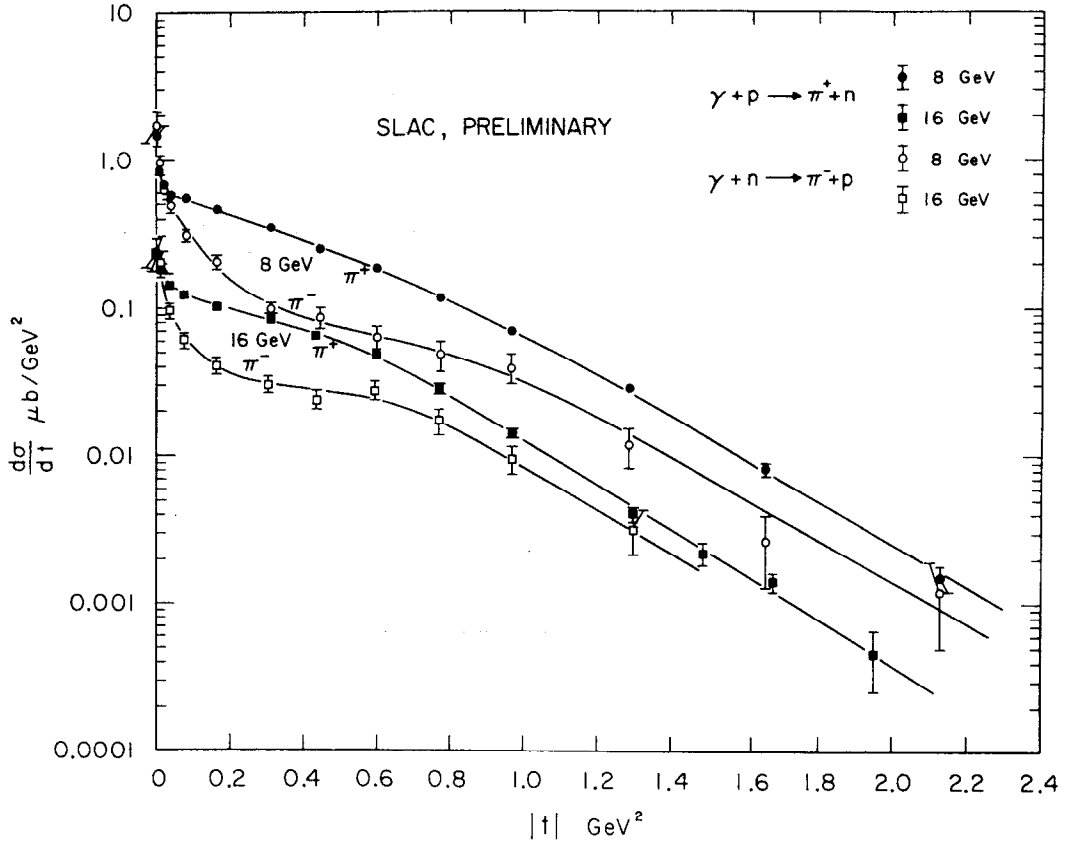
SLAC, PRELIMINARY
$\gamma + p \rightarrow \pi^+ + n$
$\gamma + n \rightarrow \pi^- + p$
8 GeV
16 GeV
8 GeV
16 GeV
8 GeV
π^+
π^-
16 GeV
π^+
π^-
$\frac{d\sigma}{dt}$ μb/GeV²
|t| GeV²

Fig. 6a

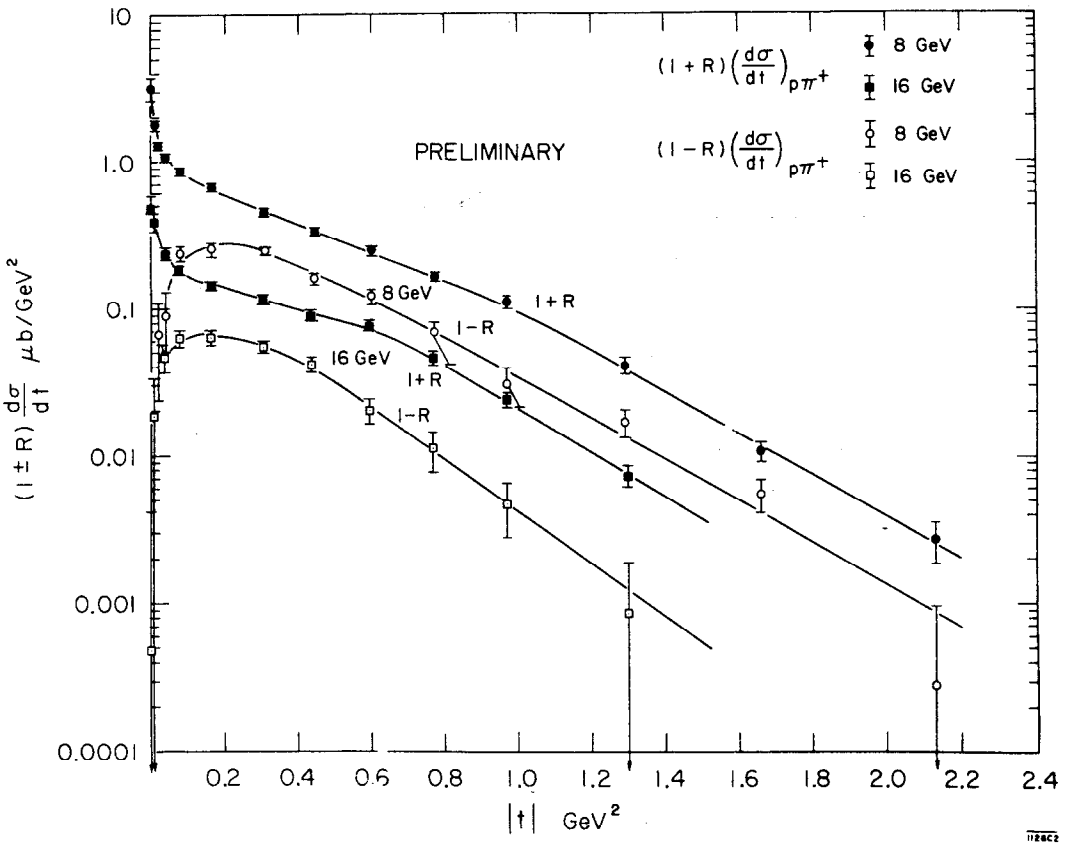
PRELIMINARY
$(1+R)\left(\frac{d\sigma}{dt}\right)_{p\pi^+}$
$(1-R)\left(\frac{d\sigma}{dt}\right)_{p\pi^+}$
8 GeV
16 GeV
8 GeV
16 GeV
8 GeV
1+R
1-R
16 GeV
1+R
1-R
$(1 \pm R)\frac{d\sigma}{dt}$ μb/GeV²
|t| GeV²

Fig. 6b

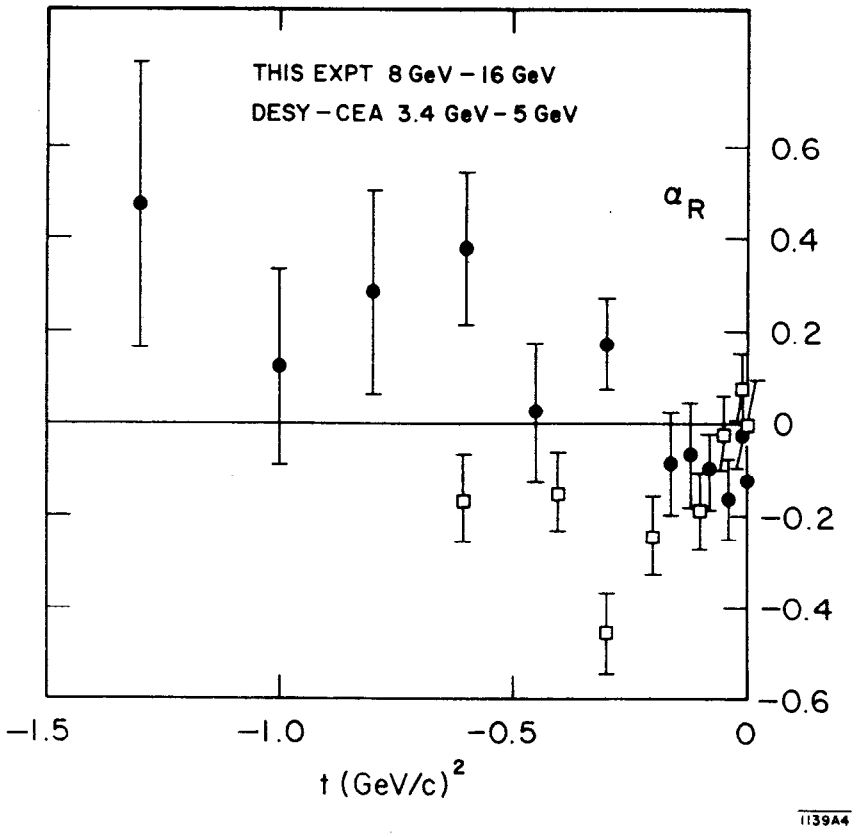
THIS EXPT 8 GeV – 16 GeV
DESY – CEA 3.4 GeV – 5 GeV
α_R
0.6
0.4
0.2
0
−0.2
−0.4
−0.6
−1.5
−1.0
−0.5
0
t (GeV/c)^2
1139A4

Fig. 7a

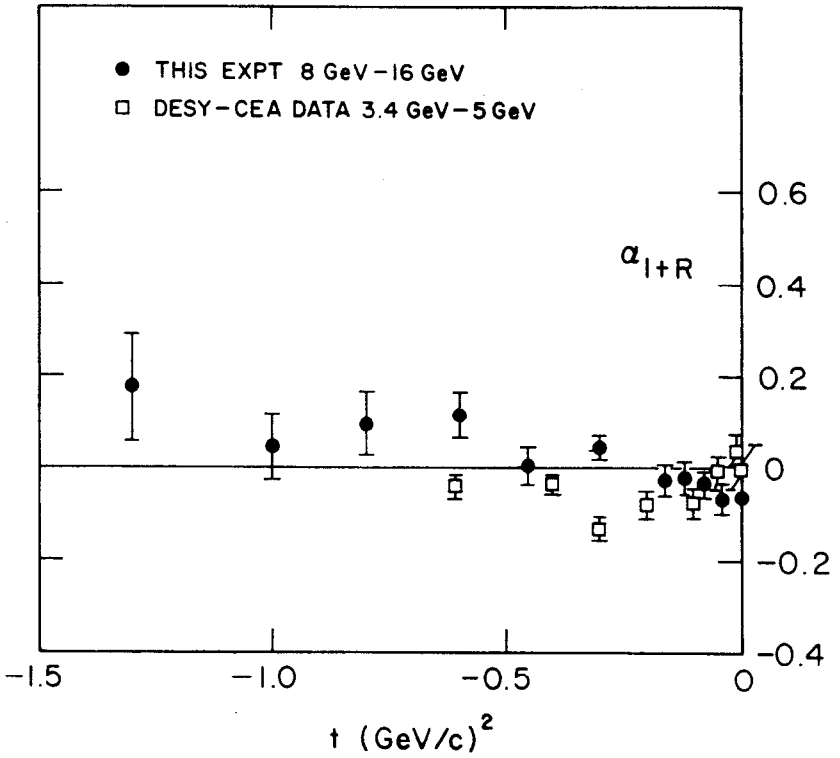
THIS EXPT 8 GeV – 16 GeV
DESY – CEA DATA 3.4 GeV – 5 GeV
α_{I+R}
0.6
0.4
0.2
0
−0.2
−0.4
−1.5
−1.0
−0.5
0
t (GeV/c)^2

Fig. 7b

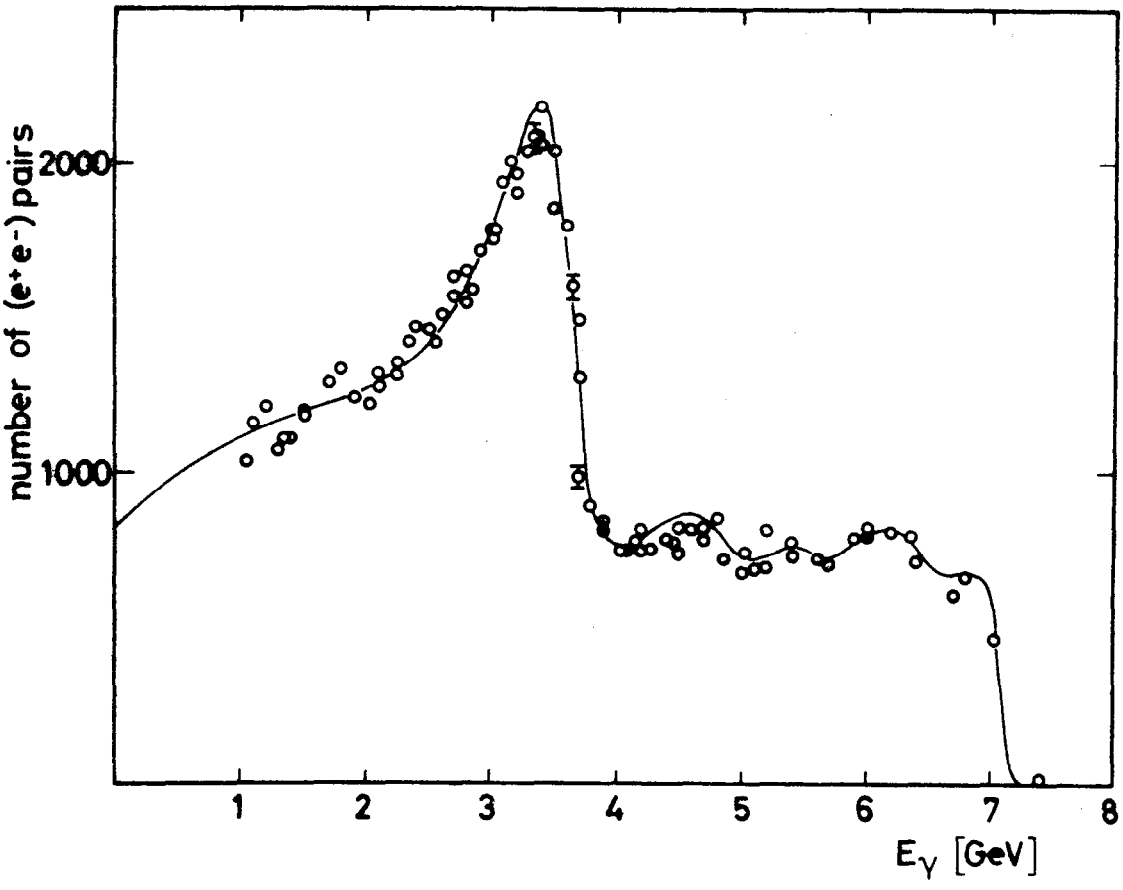
number of (e⁺e⁻) pairs
2000
1000
1
2
3
4
5
6
7
8
Eγ [GeV]

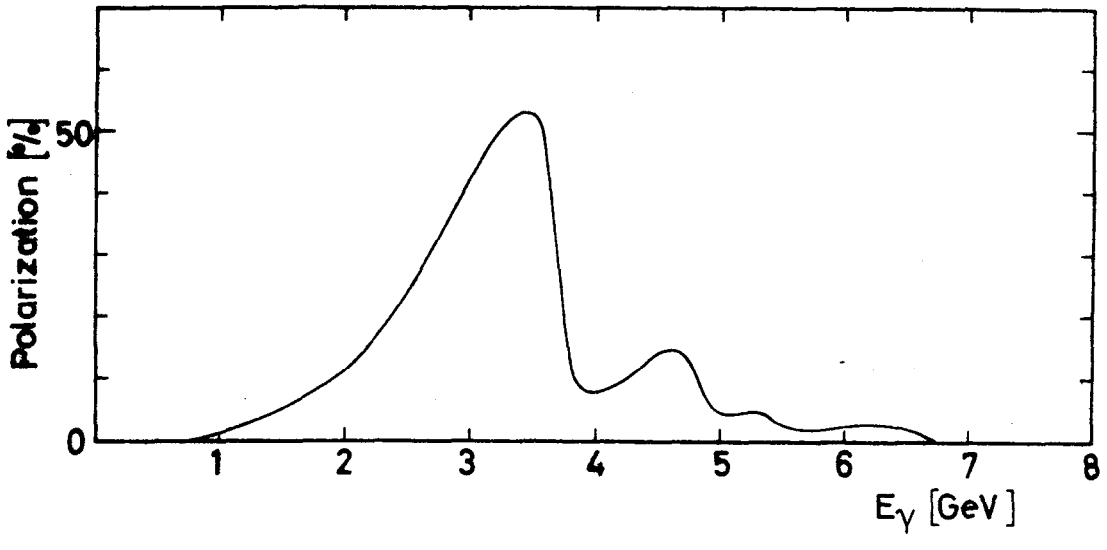
Polarization [%]
50
0
1
2
3
4
5
6
7
8
Eγ [GeV]

Fig. 8

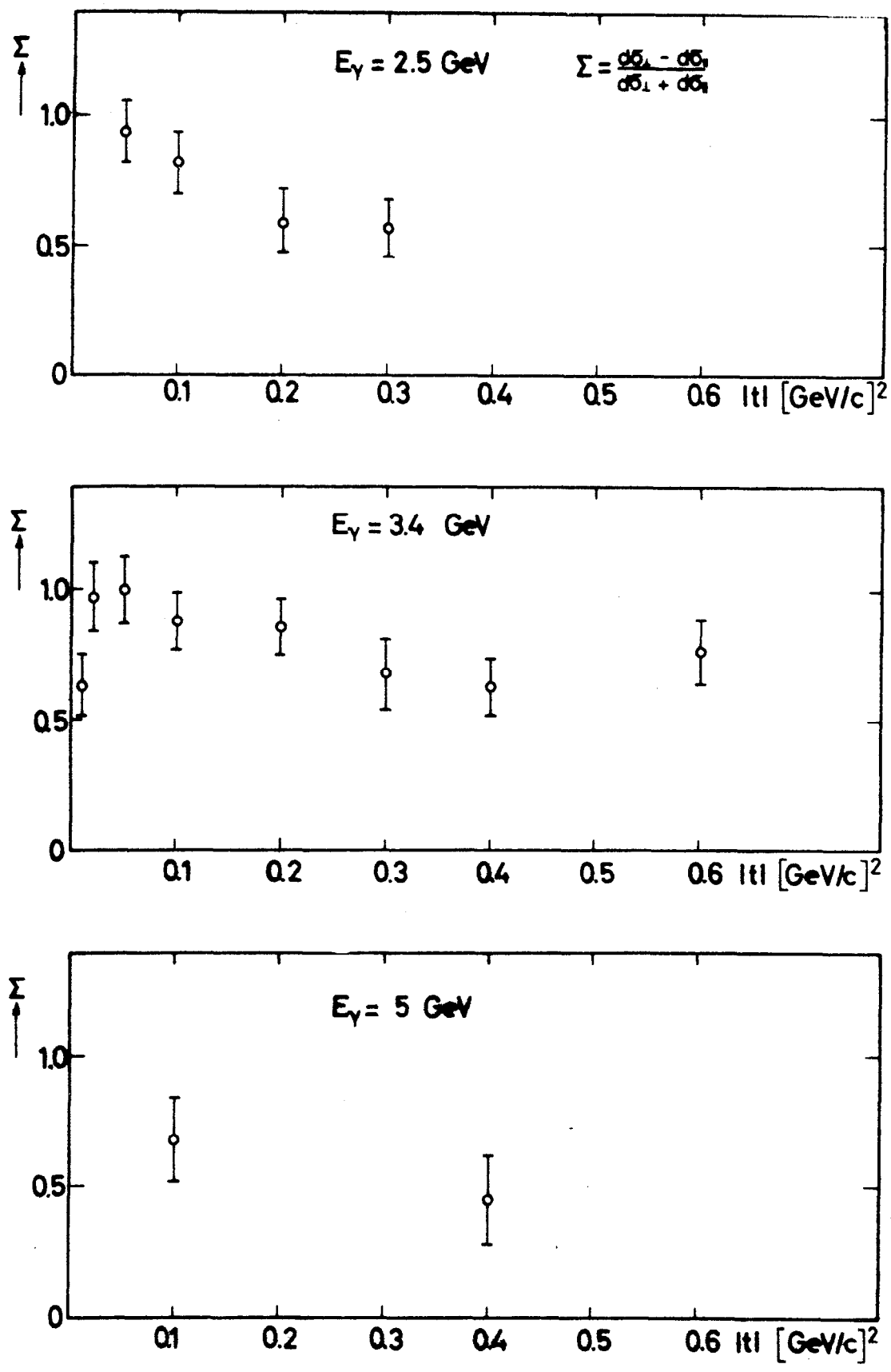
Σ
E_γ = 2.5 GeV
$\Sigma = \frac{d\sigma_\perp - d\sigma_\parallel}{d\sigma_\perp + d\sigma_\parallel}$
1.0
0.5
0
0.1
0.2
0.3
0.4
0.5
0.6 |t| [GeV/c]^2
Σ
E_γ = 3.4 GeV
1.0
0.5
0
0.1
0.2
0.3
0.4
0.5
0.6 |t| [GeV/c]^2
Σ
E_γ = 5 GeV
1.0
0.5
0
0.1
0.2
0.3
0.4
0.5
0.6 |t| [GeV/c]^2

Fig. 9

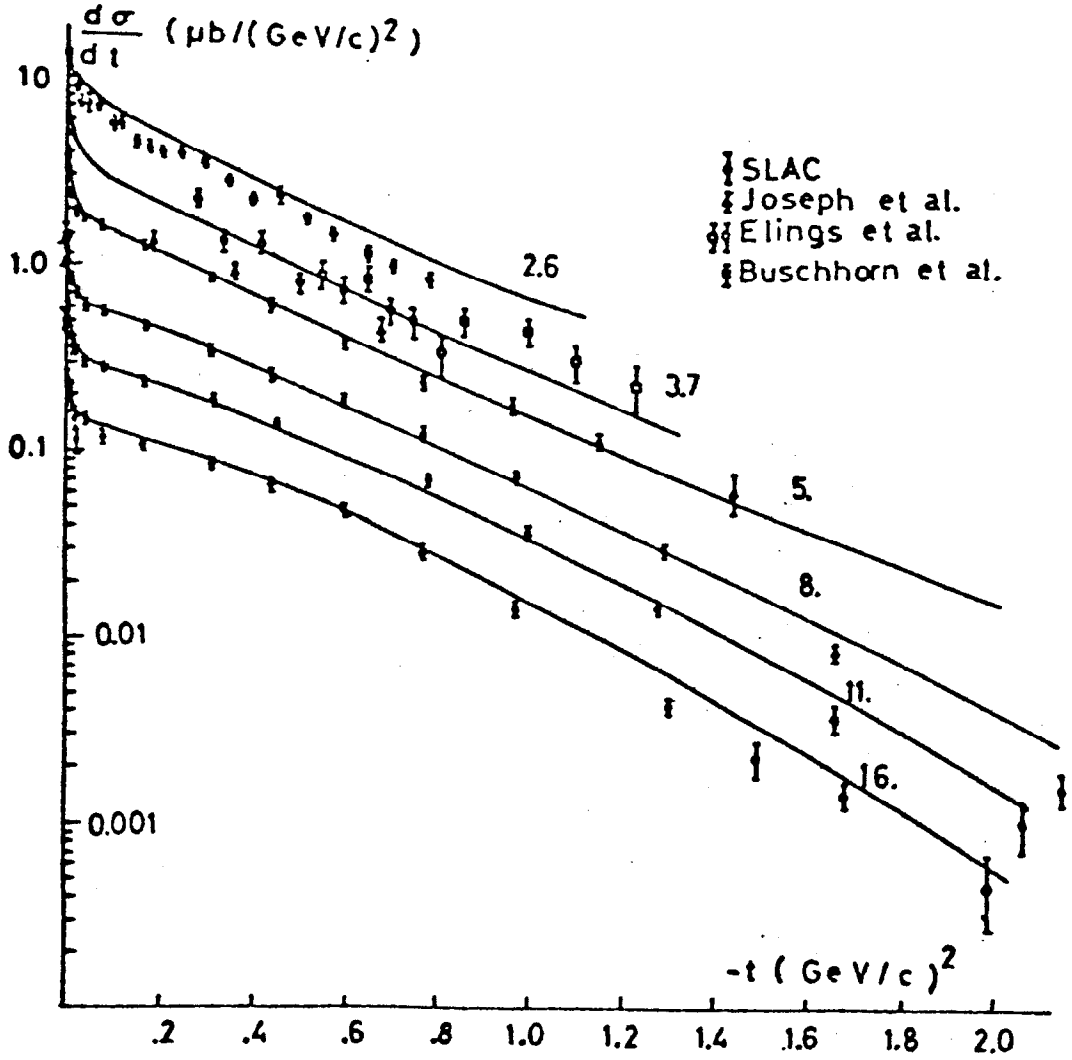
dσ/dt (μb/(GeV/c)²)
10
1.0
0.1
0.01
0.001
SLAC
Joseph et al.
Elings et al.
Buschhorn et al.
2.6
3.7
5.
8.
11.
16.
-t (GeV/c)²
.2
.4
.6
.8
1.0
1.2
1.4
1.6
1.8
2.0

Fig. 10

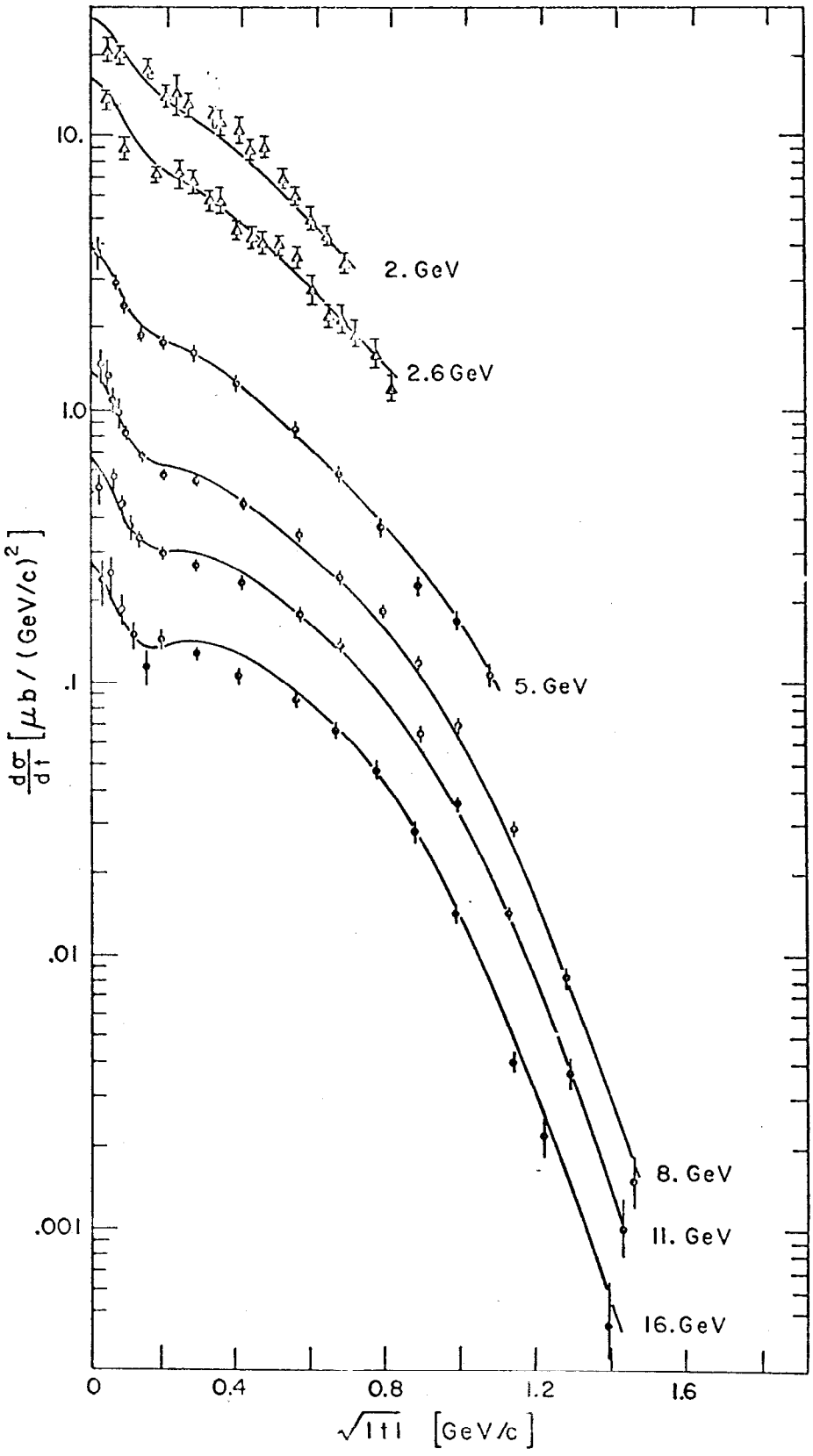
10.
1.0
.1
.01
.001
$\frac{d\sigma}{dt}$ [μb / (GeV/c)^2]
2. GeV
2.6 GeV
5. GeV
8. GeV
11. GeV
16. GeV
0
0.4
0.8
1.2
1.6
$\sqrt{|t|}$ [GeV/c]

Fig. 11

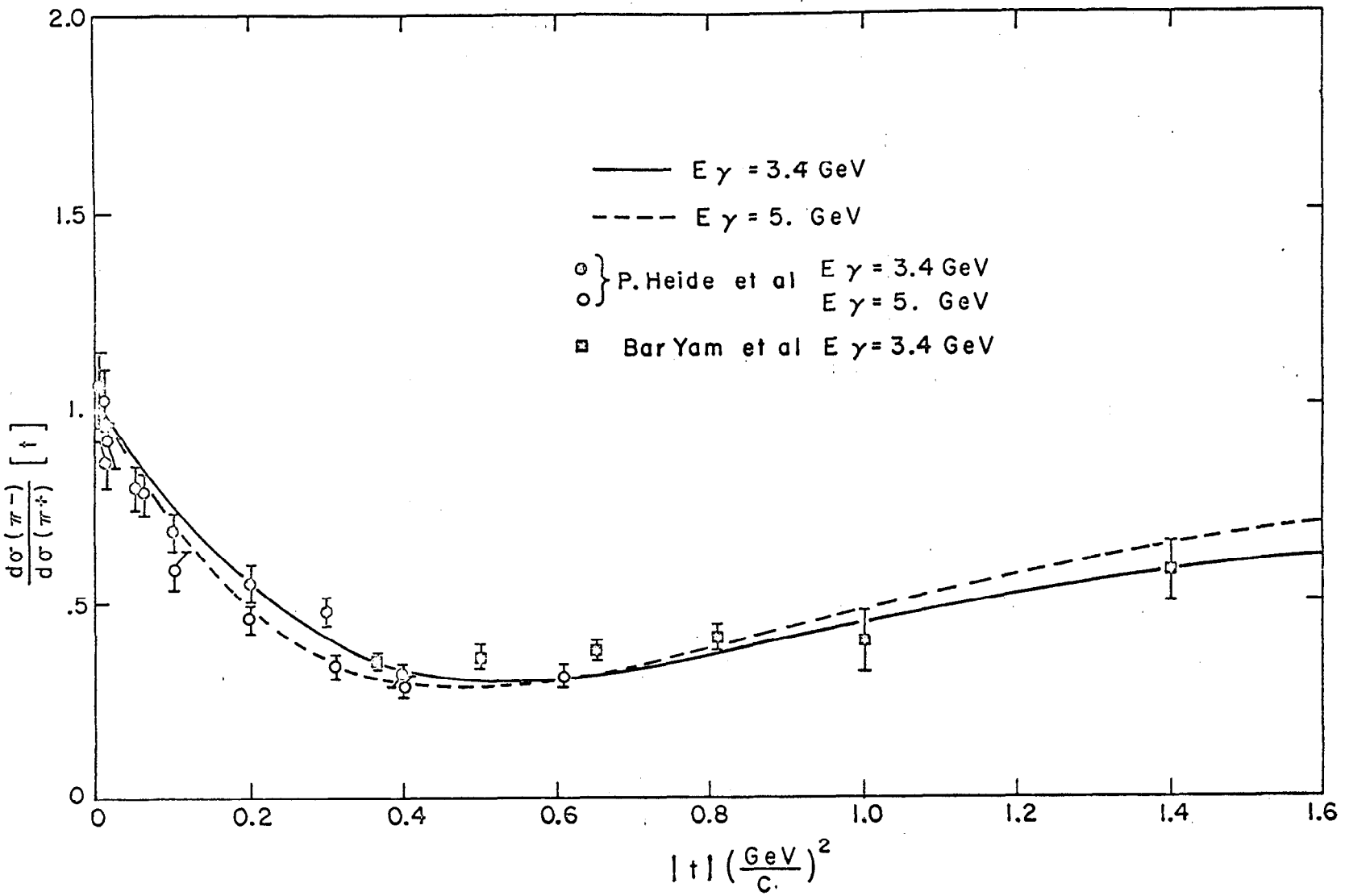
2.0
1.5
1.
.5
0
0
0.2
0.4
0.6
0.8
1.0
1.2
1.4
1.6
Eγ = 3.4 GeV
Eγ = 5. GeV
P. Heide et al Eγ = 3.4 GeV
Eγ = 5. GeV
Bar Yam et al Eγ = 3.4 GeV
dσ(π−)/dσ(π+) [t]
|t| (GeV/c)²

Fig. 12

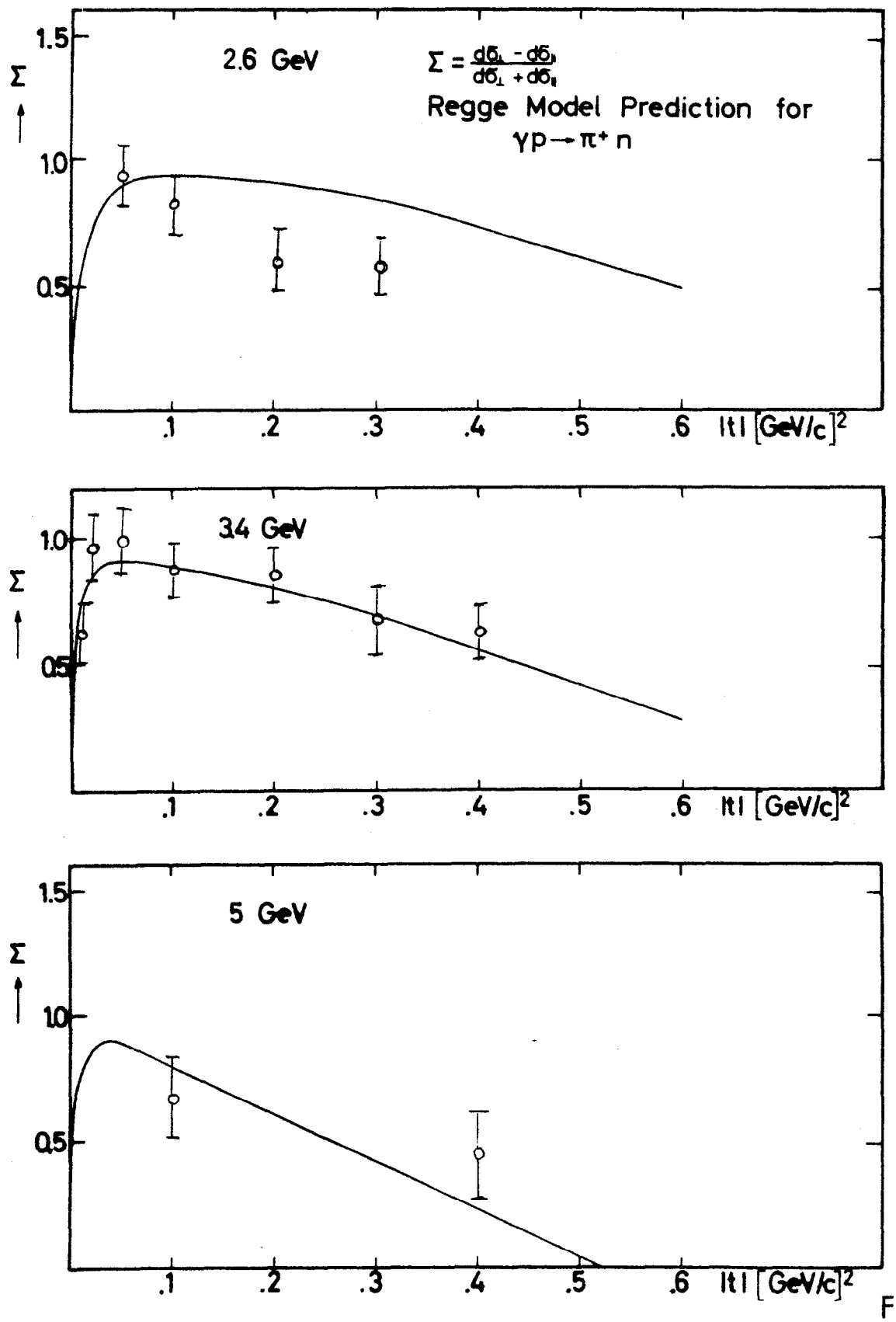
2.6 GeV
$\Sigma = \frac{d\sigma_\perp - d\sigma_\parallel}{d\sigma_\perp + d\sigma_\parallel}$
Regge Model Prediction for
$\gamma p \to \pi^+ n$
3.4 GeV
5 GeV
Σ
1.5
1.0
0.5
.1
.2
.3
.4
.5
.6
|t| [GeV/c]²

Fig. 13

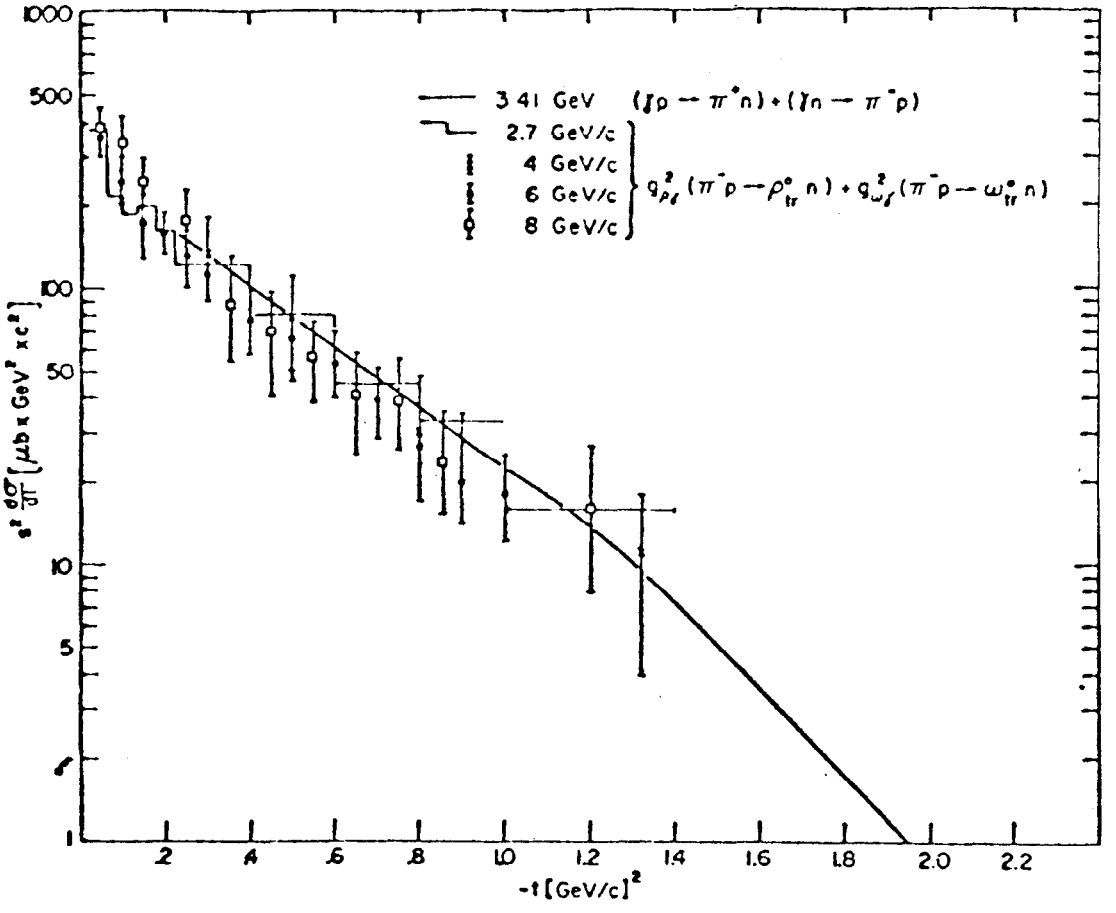

A comparison between the sum rule (7a) and experiments. The smooth line represents the sum of the experimental cross sections for $\gamma p \to \pi^+ n$ and $\gamma n \to \pi^- p$. It was determined from the $\gamma p \to \pi^+ n$ cross section given in Ref. 8 and with the measured π^-/π^+ ratio of Ref. 9. The experimental results for the ρ and ω differential cross section and density matrix were taken from Refs. 7 and 12. The experimental average values $g_{\rho\gamma}{}^2 = 4.6 \times 10^{-3}$, $g_{\omega\gamma}{}^2 = 6.6 \times 10^{-4}$ were taken from Ref. 6.

Fig. 14

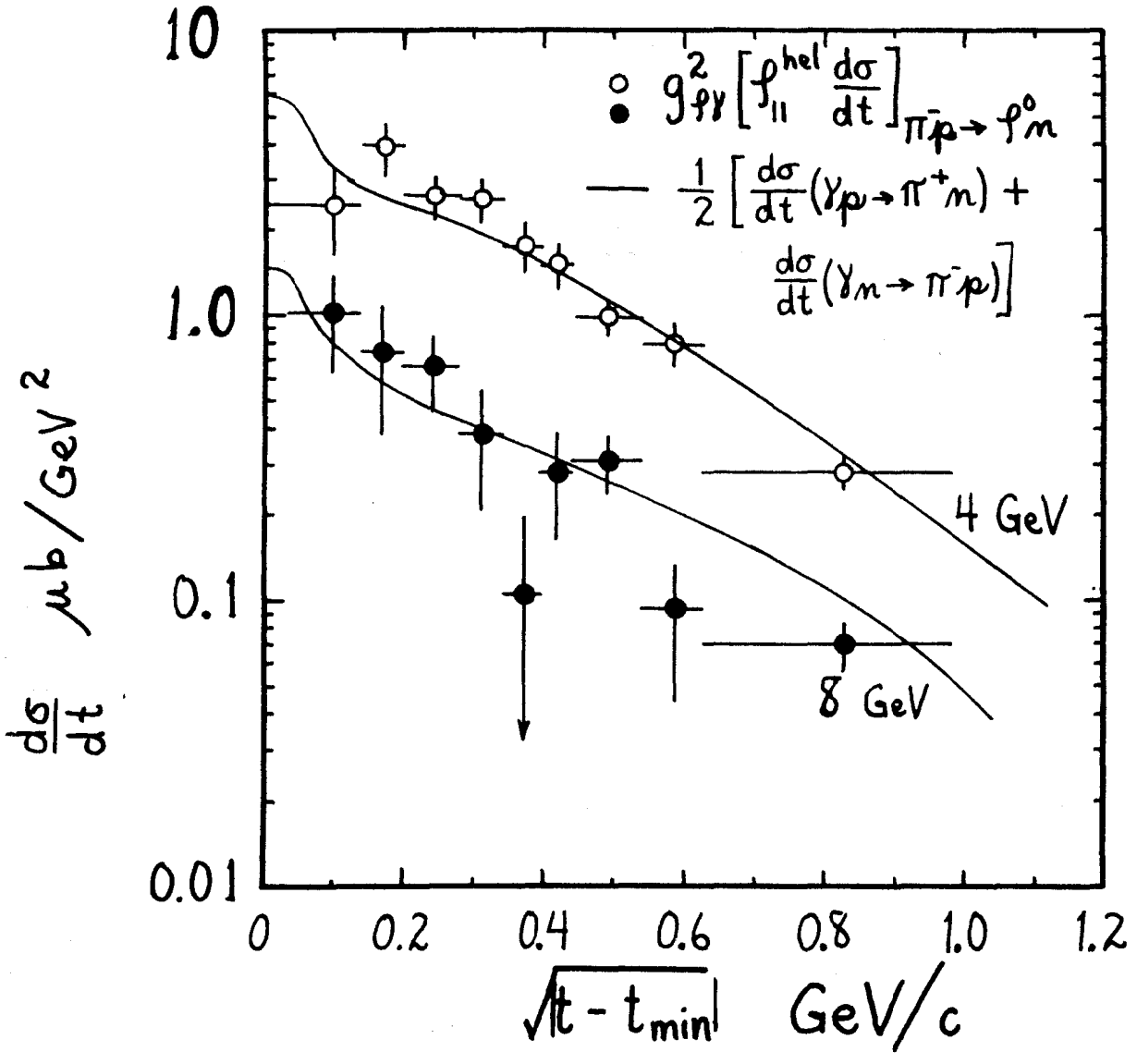
10
1.0
0.1
0.01
0
0.2
0.4
0.6
0.8
1.0
1.2
$g^2_{f\gamma}\left[\rho^{hel}_{11}\frac{d\sigma}{dt}\right]_{\pi^-p\to\rho^0 n}$
$\frac{1}{2}\left[\frac{d\sigma}{dt}(\gamma p\to\pi^+ n)+\frac{d\sigma}{dt}(\gamma n\to\pi^- p)\right]$
4 GeV
8 GeV
$\frac{d\sigma}{dt}$ μb/GeV²
$\sqrt{|t-t_{min}|}$ GeV/c

Fig. 15

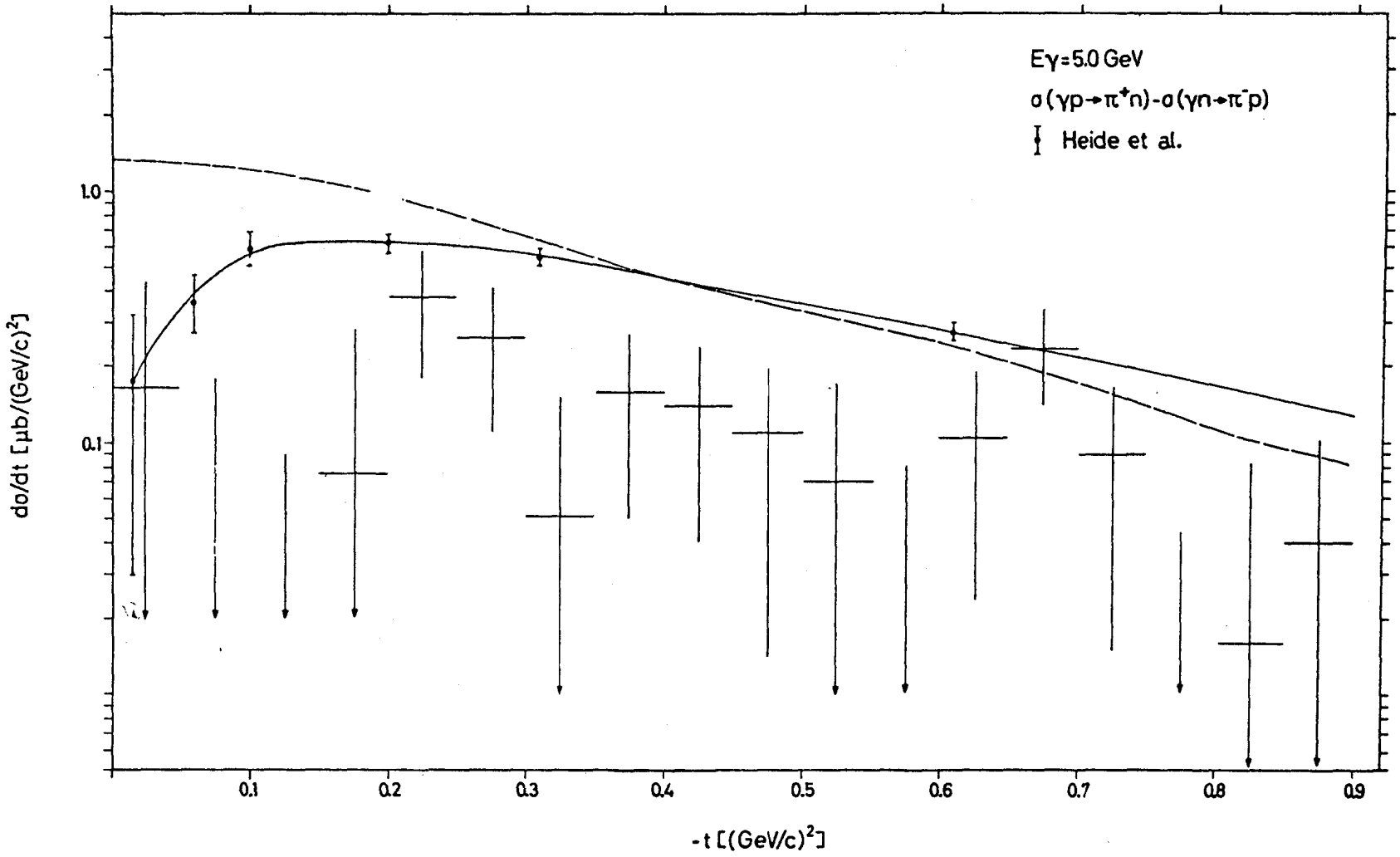
Eγ=5.0 GeV
σ(γp→π⁺n)-σ(γn→π⁻p)
Heide et al.
dσ/dt [μb/(GeV/c)²]
1.0
0.1
0.1
0.2
0.3
0.4
0.5
0.6
0.7
0.8
0.9
-t [(GeV/c)²]

Fig. 16

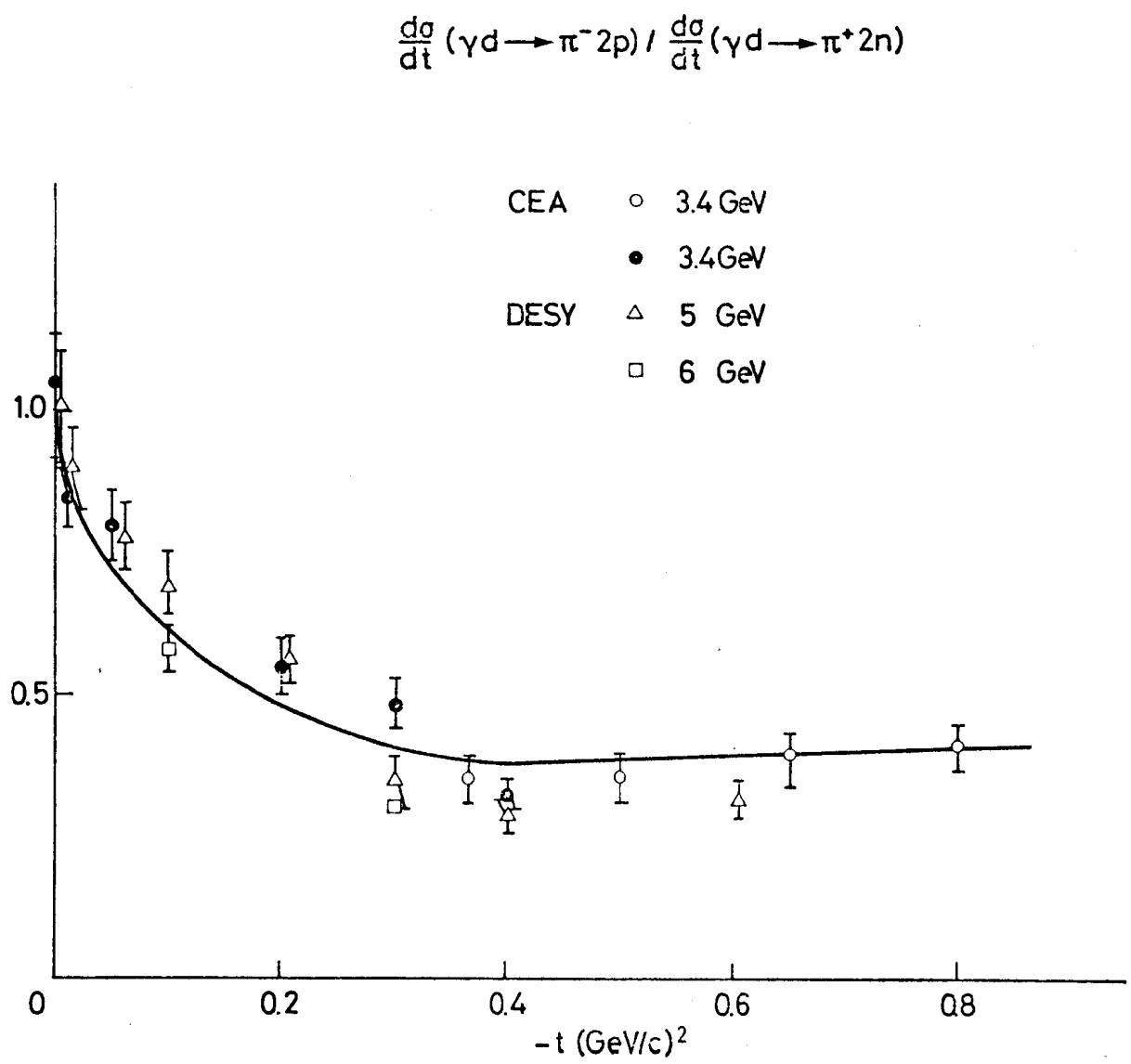
$\frac{d\sigma}{dt}(\gamma d \rightarrow \pi^- 2p) / \frac{d\sigma}{dt}(\gamma d \rightarrow \pi^+ 2n)$
CEA
3.4 GeV
3.4GeV
DESY
5 GeV
6 GeV
1.0
0.5
0
0.2
0.4
0.6
0.8
$-t\ (GeV/c)^2$

Fig. 17

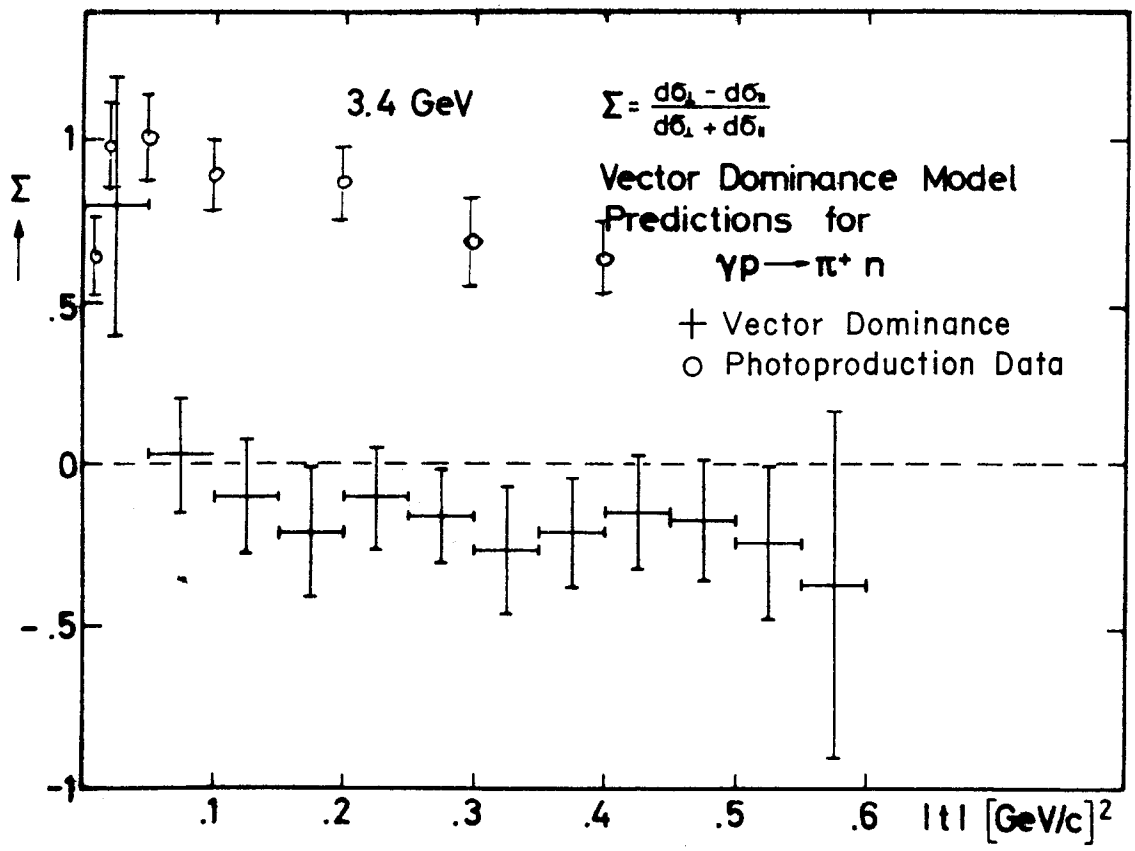
3.4 GeV
$\Sigma = \frac{d\sigma_\perp - d\sigma_\parallel}{d\sigma_\perp + d\sigma_\parallel}$
Vector Dominance Model
Predictions for
$\gamma p \rightarrow \pi^+ n$
+ Vector Dominance
o Photoproduction Data
Σ
1
.5
0
-.5
-1
.1
.2
.3
.4
.5
.6
|t| [GeV/c]²

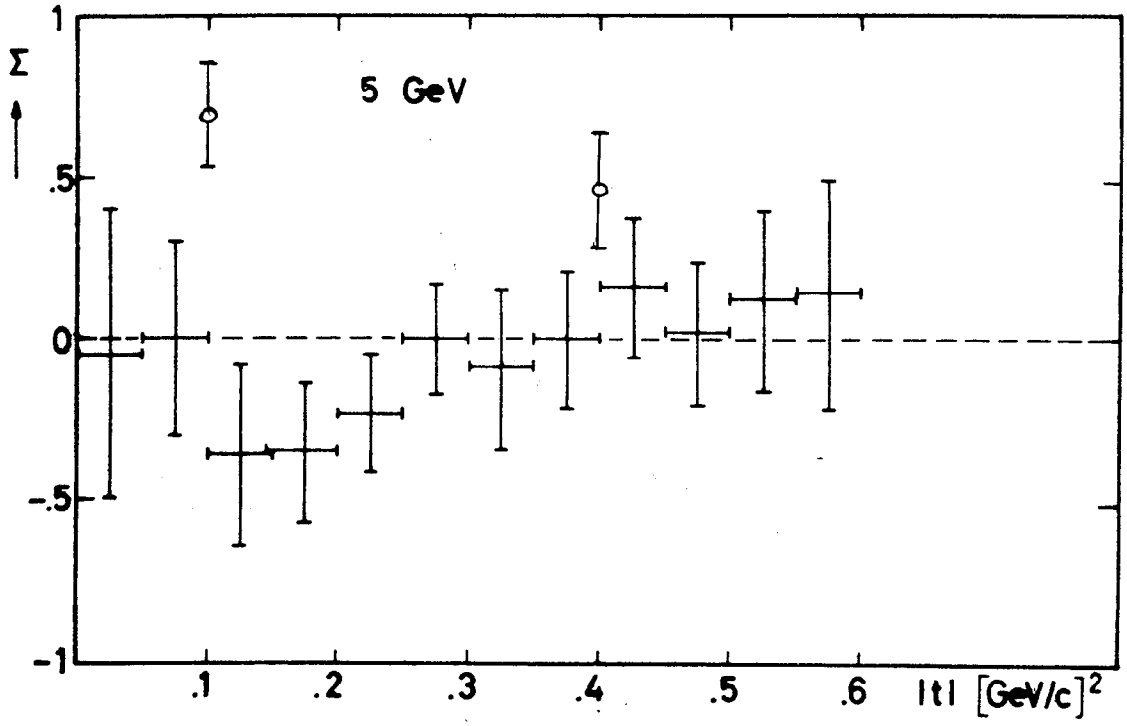
5 GeV
Σ
1
.5
0
-.5
-1
.1
.2
.3
.4
.5
.6
|t| [GeV/c]²

Fig. 18

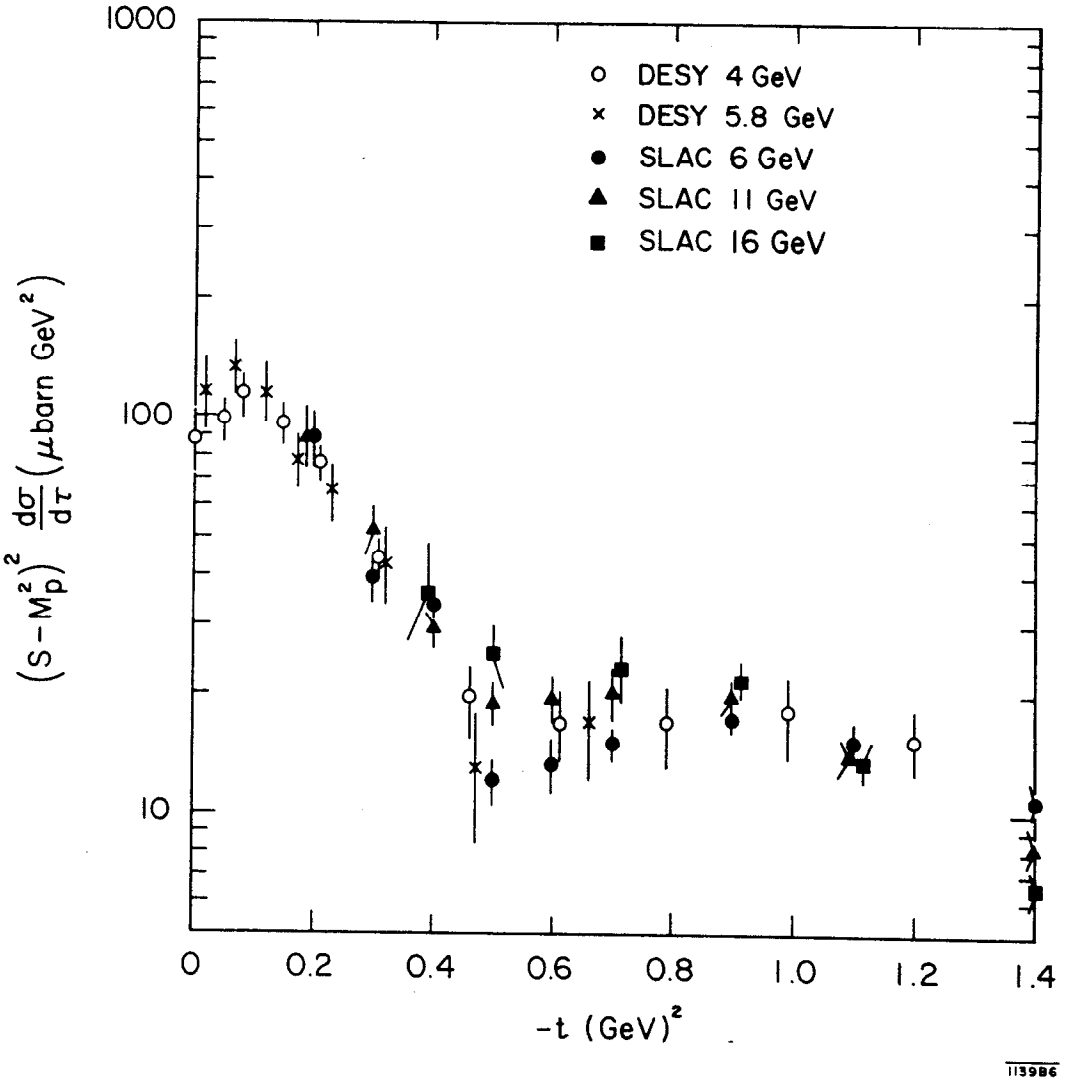
1000
100
10
0
0.2
0.4
0.6
0.8
1.0
1.2
1.4
DESY 4 GeV
DESY 5.8 GeV
SLAC 6 GeV
SLAC 11 GeV
SLAC 16 GeV
$(S-M_p^2)^2 \frac{d\sigma}{dt}$ (μbarn GeV^2)
$-t$ (GeV)^2
1139B6

Fig. 19

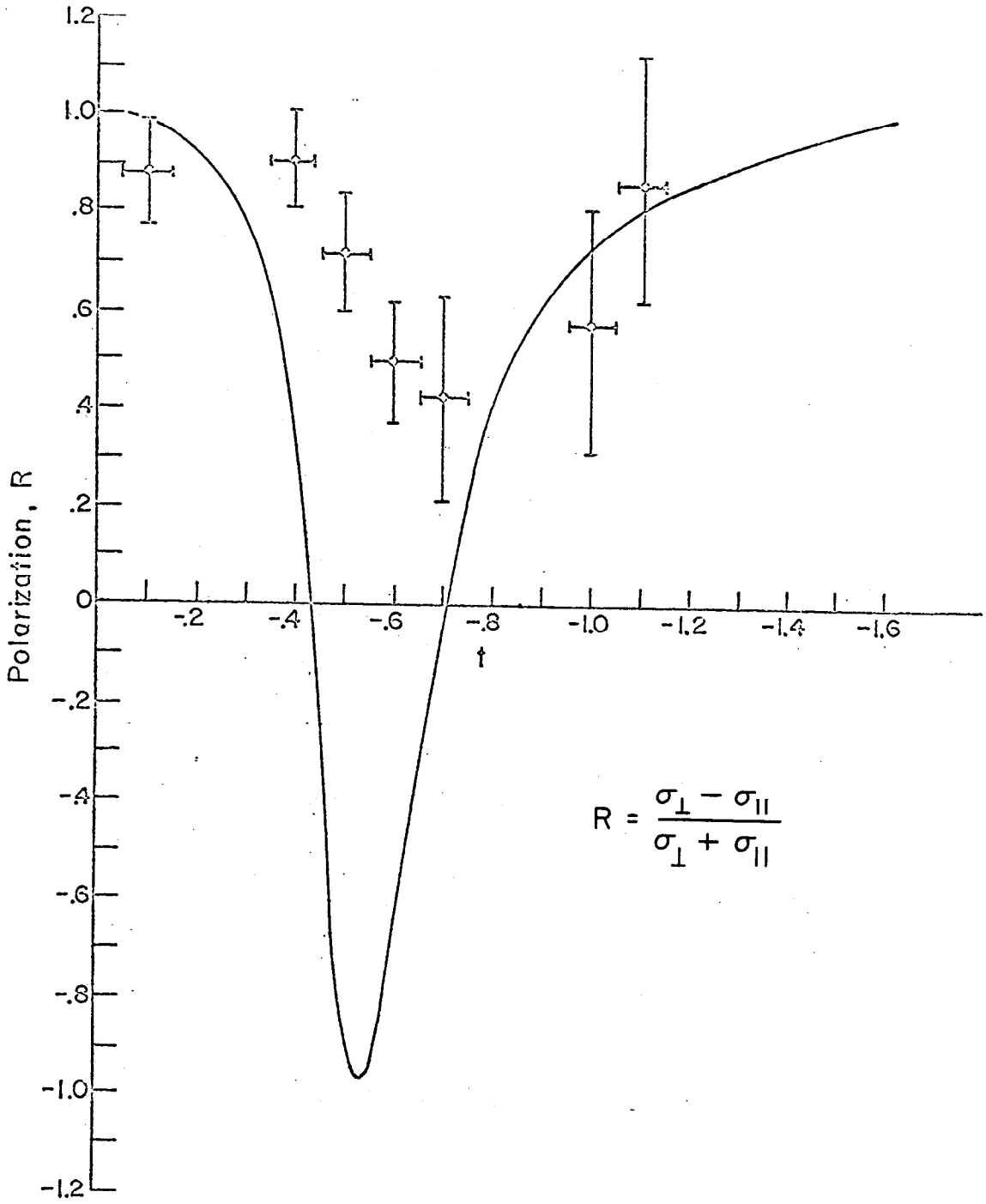
1.2
1.0
.8
.6
.4
.2
0
-.2
-.4
-.6
-.8
-1.0
-1.2
Polarization, R
-.2
-.4
-.6
-.8
-1.0
-1.2
-1.4
-1.6
t
$R = \frac{\sigma_\perp - \sigma_{||}}{\sigma_\perp + \sigma_{||}}$

Fig. 20

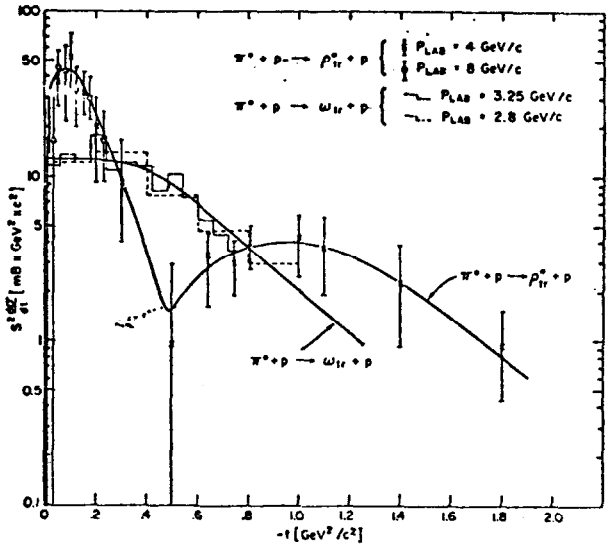

Fig. 21a

Cross section $s^2(d\sigma/dt)$ for $\pi^0 p \rightarrow \rho_{tr}{}^0 p$ and $\pi^0 p \rightarrow \omega_{tr} p$ as determined from (9a) and (9b). The experimental points were taken from Ref. 7. ρ_{00} was taken to be s independent as indicated by the low-energy data. The smooth lines are interpolating lines through the experimental points.

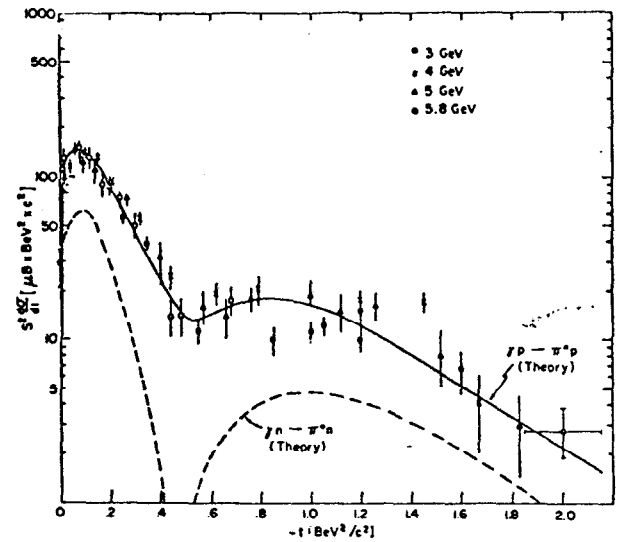

Fig. 21b

Comparison between experimental cross sections $s^2(d\sigma/dt)$ of Ref. 10 for π^0 photoproduction and theoretical predictions obtained by substituting into Eq. (8a) the experimental average values $g_{\rho\gamma}{}^2 = 4.6 \times 10^{-3}$, $g_{\omega\rho}{}^2 = 6.6 \times 10^{-4}$ of Ref. 6 and experimental cross sections (Ref. 9) from curves drawn through the experimental points of Fig. 2.

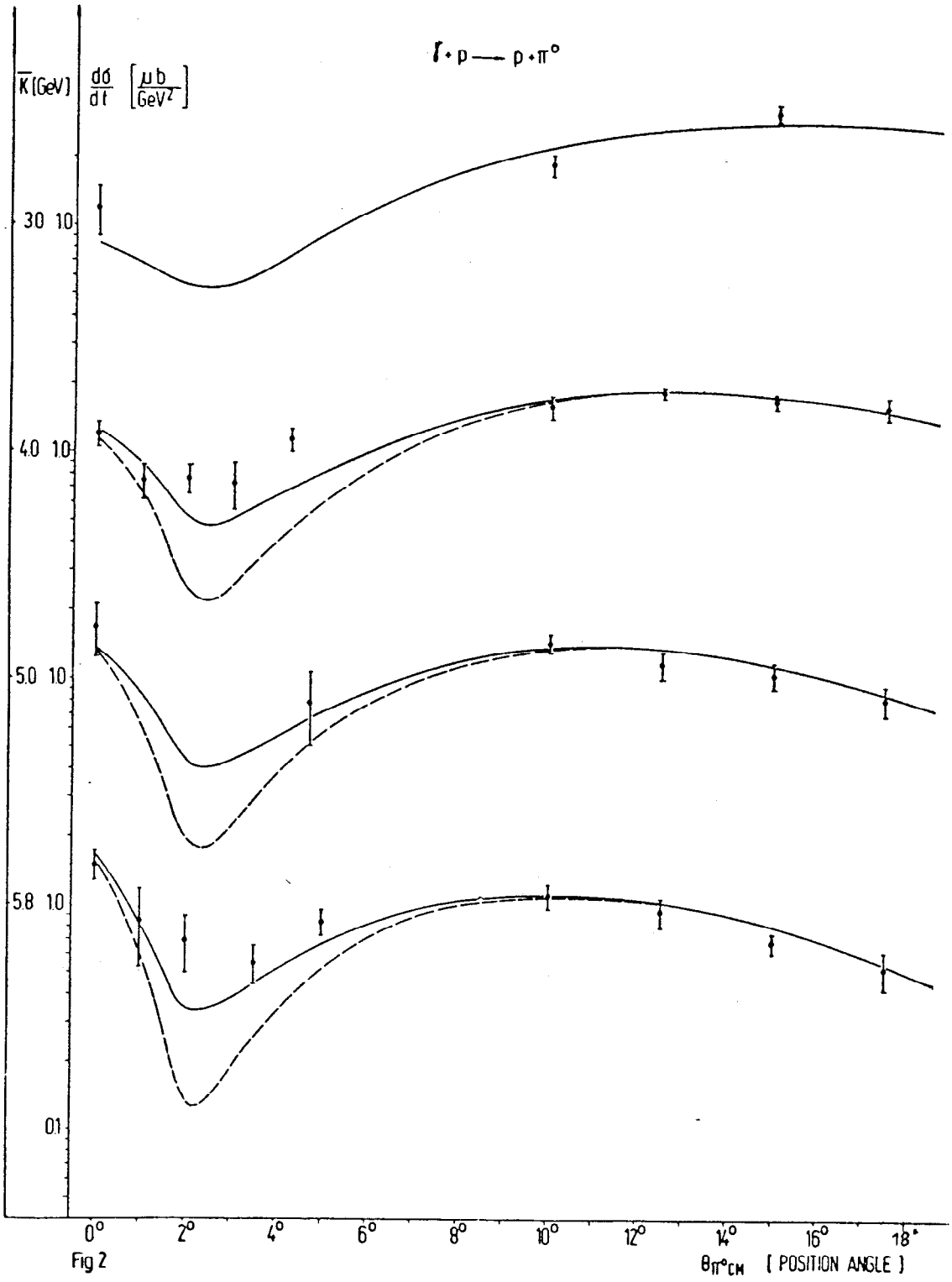
γ + p — p + π°
K̄ (GeV)
dσ/dt [μb/GeV²]
3.0 1.0
4.0 1.0
5.0 1.0
5.8 1.0
0.1
0°
2°
4°
6°
8°
10°
12°
14°
16°
18°
θπ°CM [POSITION ANGLE]

Fig 2

Fig. 22

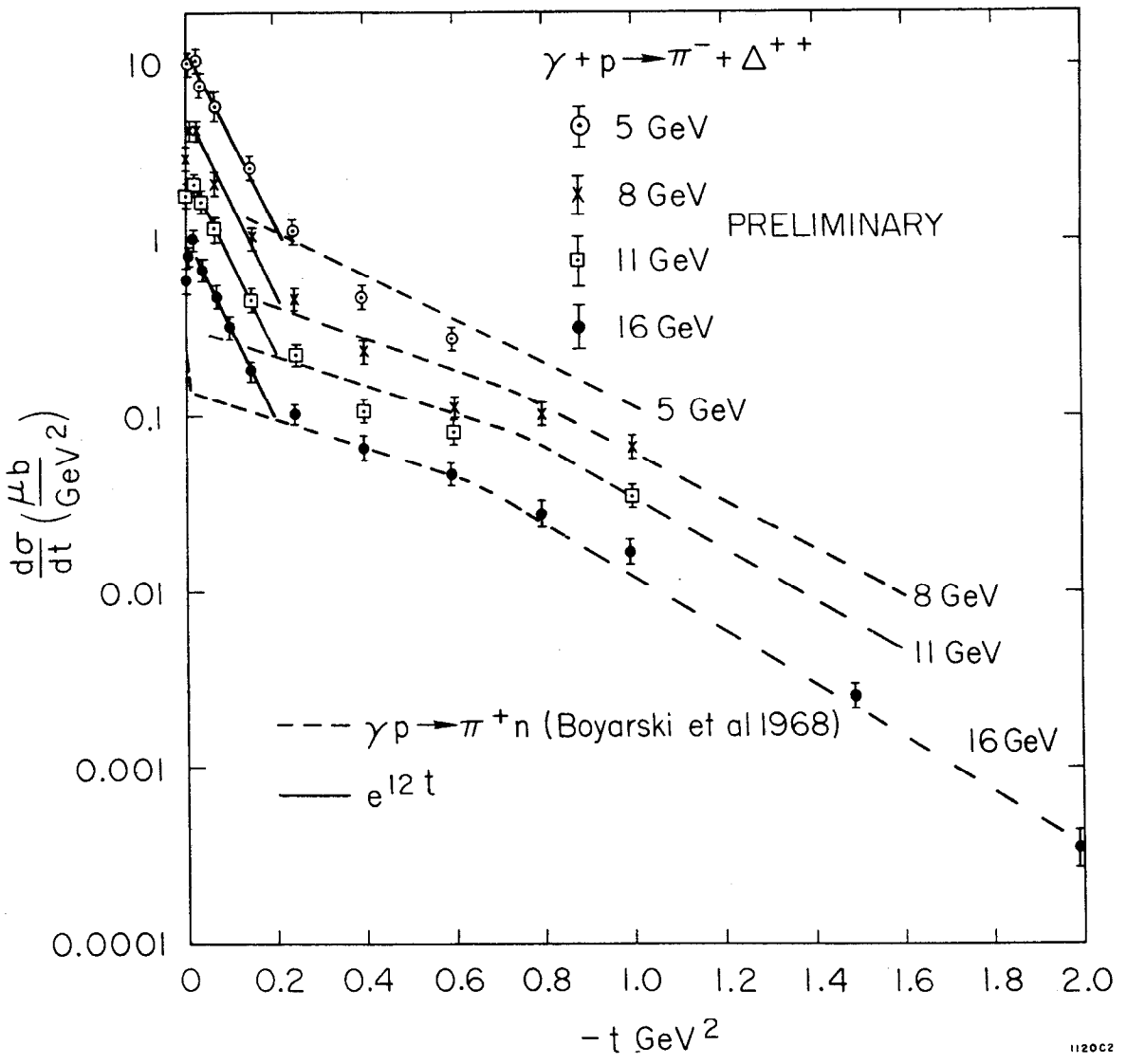
$\gamma + p \rightarrow \pi^- + \Delta^{++}$
5 GeV
8 GeV
11 GeV
16 GeV
PRELIMINARY
5 GeV
8 GeV
11 GeV
16 GeV
$\gamma p \rightarrow \pi^+ n$ (Boyarski et al 1968)
e^{12t}
$\frac{d\sigma}{dt}\left(\frac{\mu b}{GeV^2}\right)$
$-t\ GeV^2$
10
1
0.1
0.01
0.001
0.0001
0
0.2
0.4
0.6
0.8
1.0
1.2
1.4
1.6
1.8
2.0
112062

Fig. 23

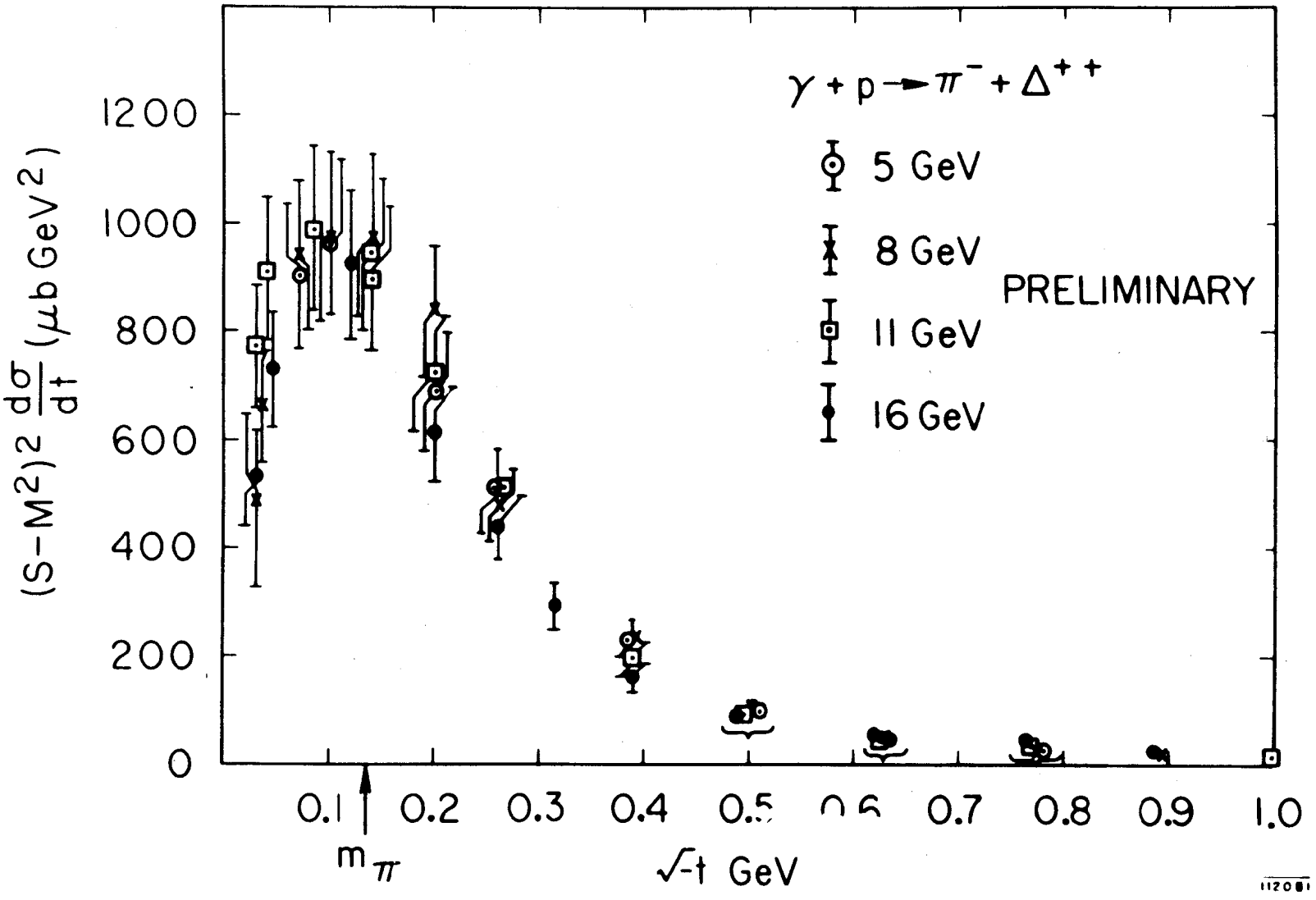
$\gamma + p \rightarrow \pi^- + \Delta^{++}$
5 GeV
8 GeV
11 GeV
16 GeV
PRELIMINARY
$(S-M^2)^2 \frac{d\sigma}{dt}$ (μb GeV^2)
1200
1000
800
600
400
200
0
0.1
0.2
0.3
0.4
0.5
0.6
0.7
0.8
0.9
1.0
m_π
$\sqrt{-t}$ GeV

Fig. 24

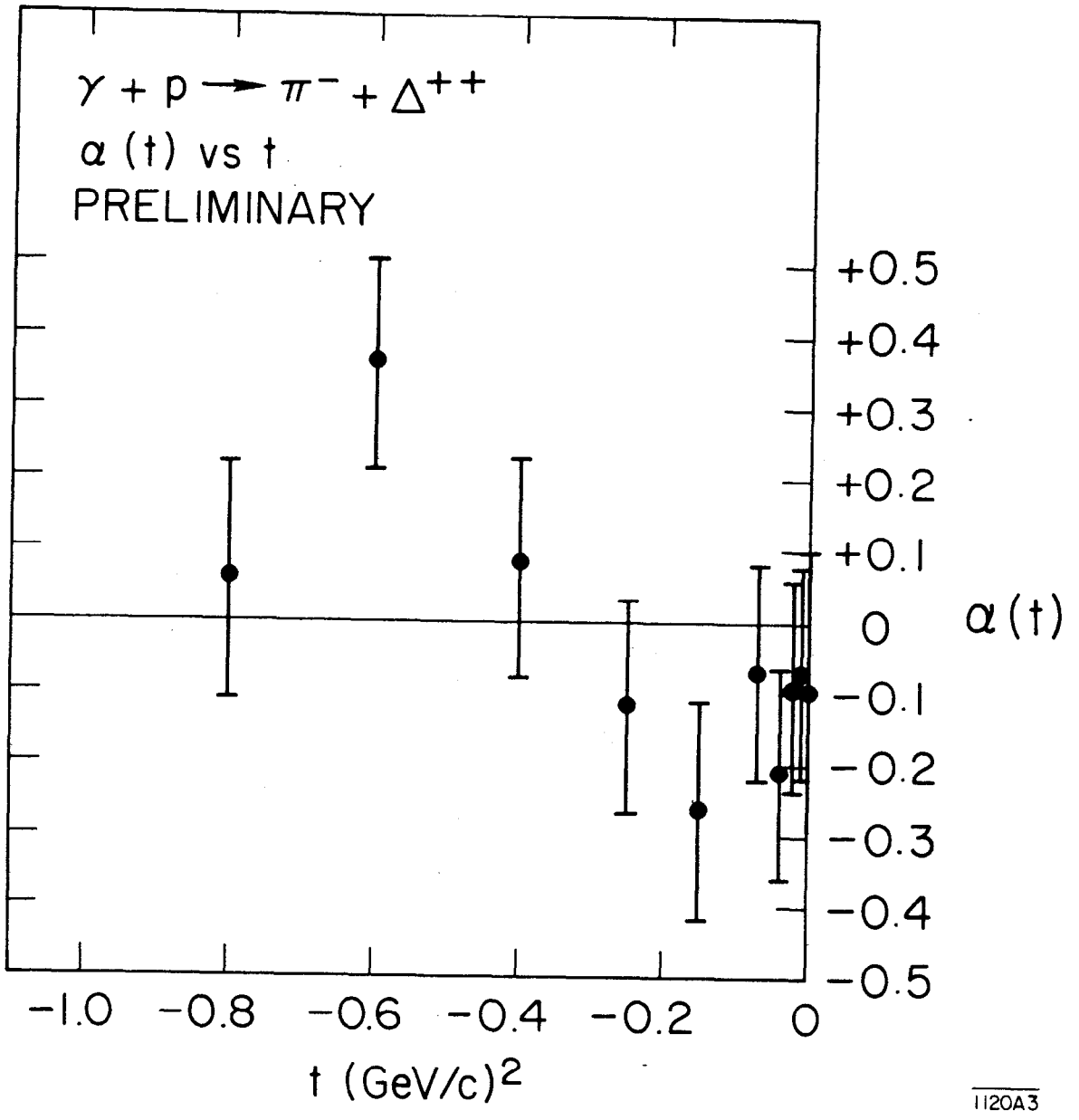
γ + p → π⁻ + Δ⁺⁺
α (t) vs t
PRELIMINARY
+0.5
+0.4
+0.3
+0.2
+0.1
0
−0.1
−0.2
−0.3
−0.4
−0.5
α(t)
−1.0
−0.8
−0.6
−0.4
−0.2
0
t (GeV/c)²
1120A3

Fig. 25

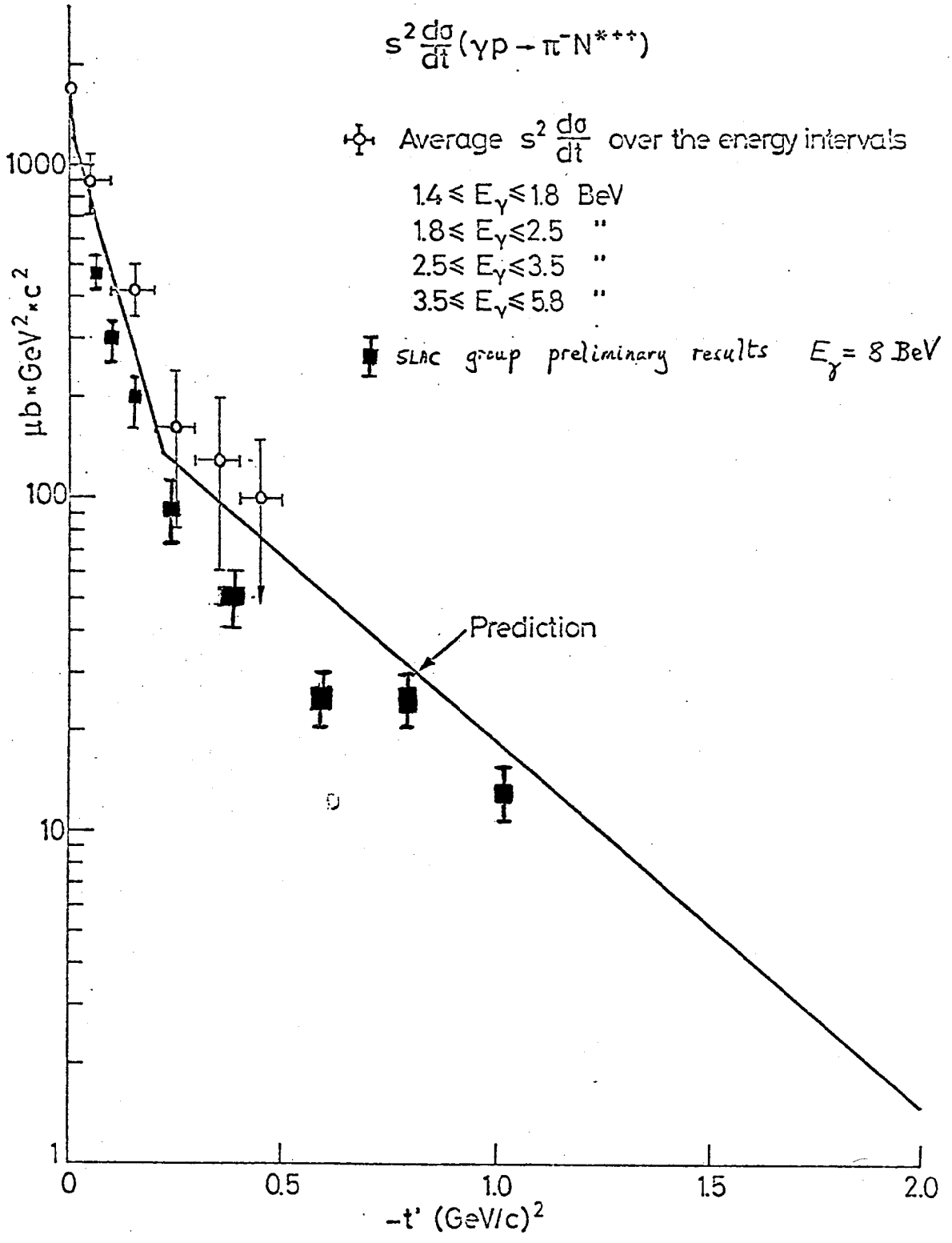
$s^2 \frac{d\sigma}{dt}(\gamma p \to \pi^- N^{***})$
Average $s^2 \frac{d\sigma}{dt}$ over the energy intervals
$1.4 \leq E_\gamma \leq 1.8$ BeV
$1.8 \leq E_\gamma \leq 2.5$ "
$2.5 \leq E_\gamma \leq 3.5$ "
$3.5 \leq E_\gamma \leq 5.8$ "
SLAC group preliminary results $E_\gamma = 8$ BeV
Prediction
$\mu b \cdot GeV^2 \cdot c^2$
1000
100
10
1
0
0.5
1.0
1.5
2.0
$-t'$ (GeV/c)^2

Fig. 26

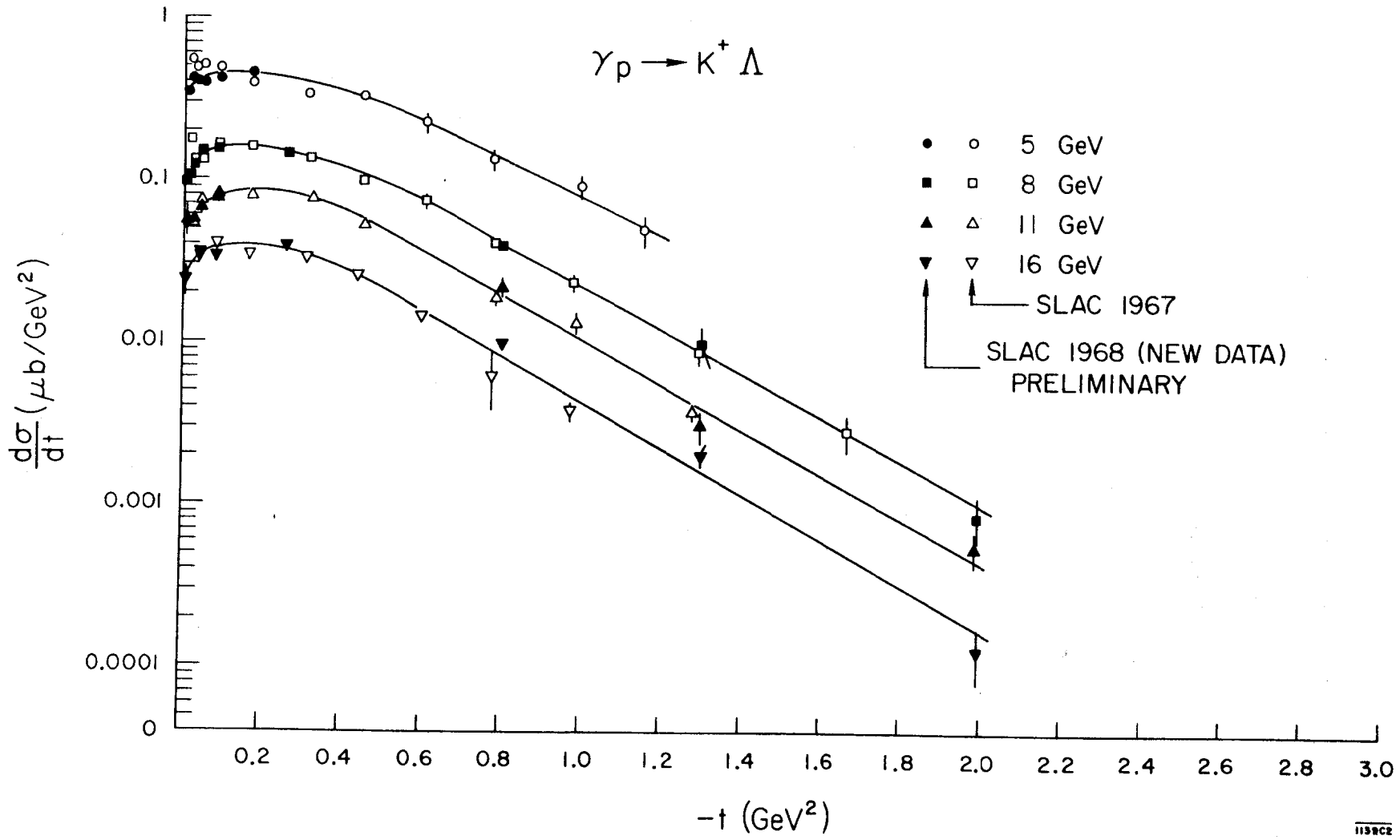
$\gamma p \rightarrow K^+ \Lambda$
5 GeV
8 GeV
11 GeV
16 GeV
SLAC 1967
SLAC 1968 (NEW DATA)
PRELIMINARY
$\frac{d\sigma}{dt}$ (μb/GeV^2)
1
0.1
0.01
0.001
0.0001
0
0.2
0.4
0.6
0.8
1.0
1.2
1.4
1.6
1.8
2.0
2.2
2.4
2.6
2.8
3.0
$-t$ (GeV^2)
113RC2

Fig. 27

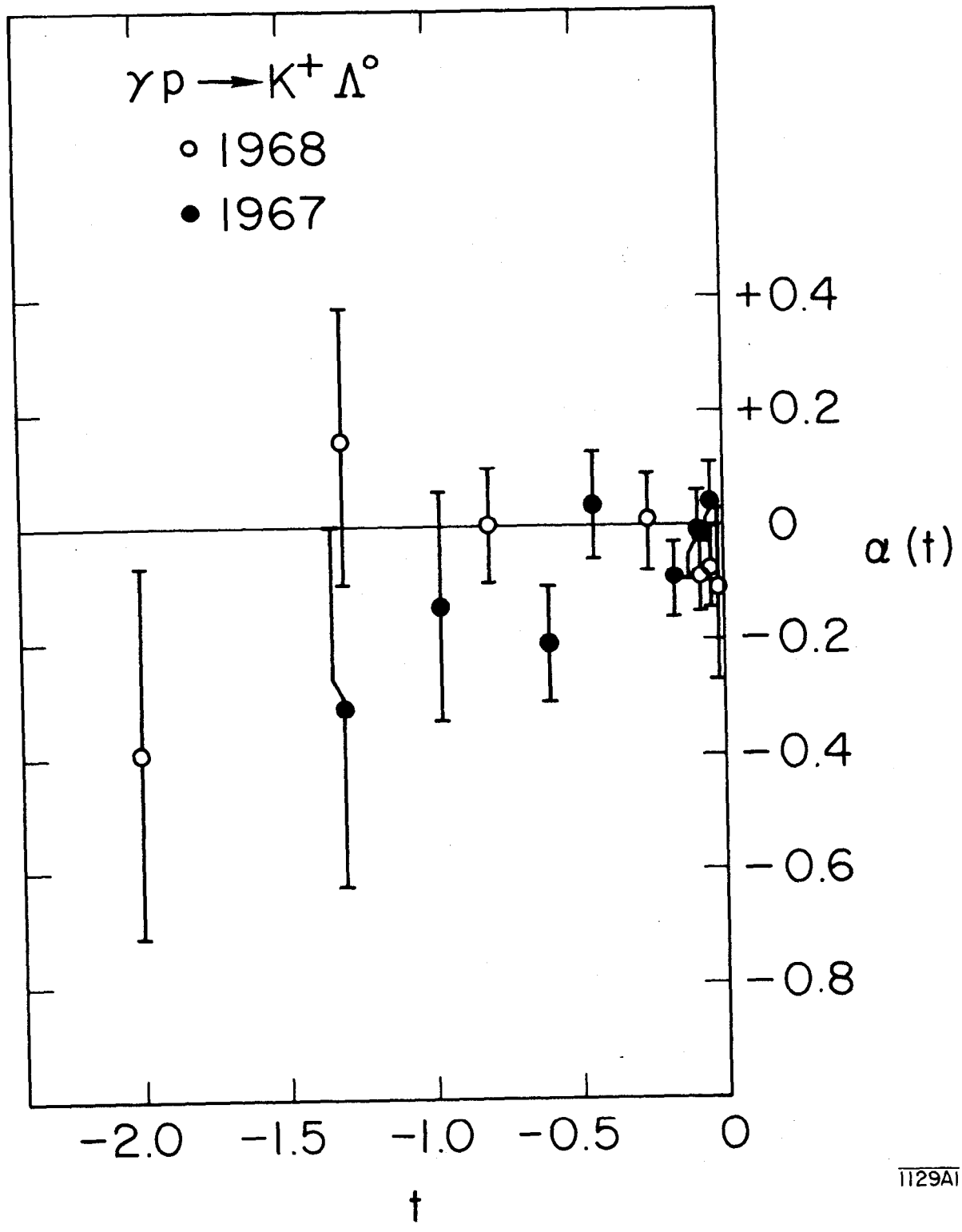

Fig. 28

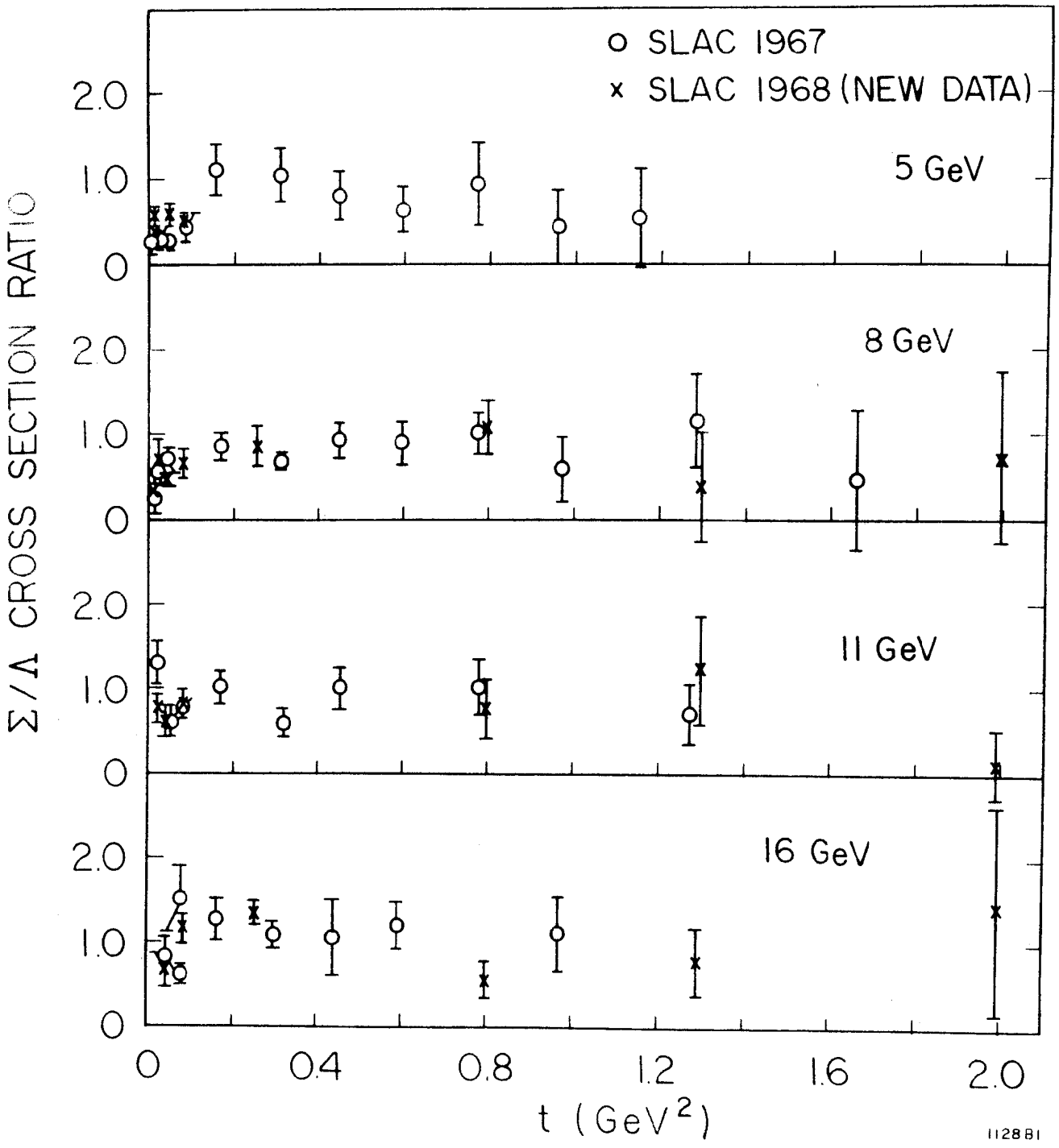
o SLAC 1967
x SLAC 1968 (NEW DATA)
5 GeV
8 GeV
11 GeV
16 GeV
Σ/Λ CROSS SECTION RATIO
t (GeV²)
0
0.4
0.8
1.2
1.6
2.0
1.0
112881

Fig. 29

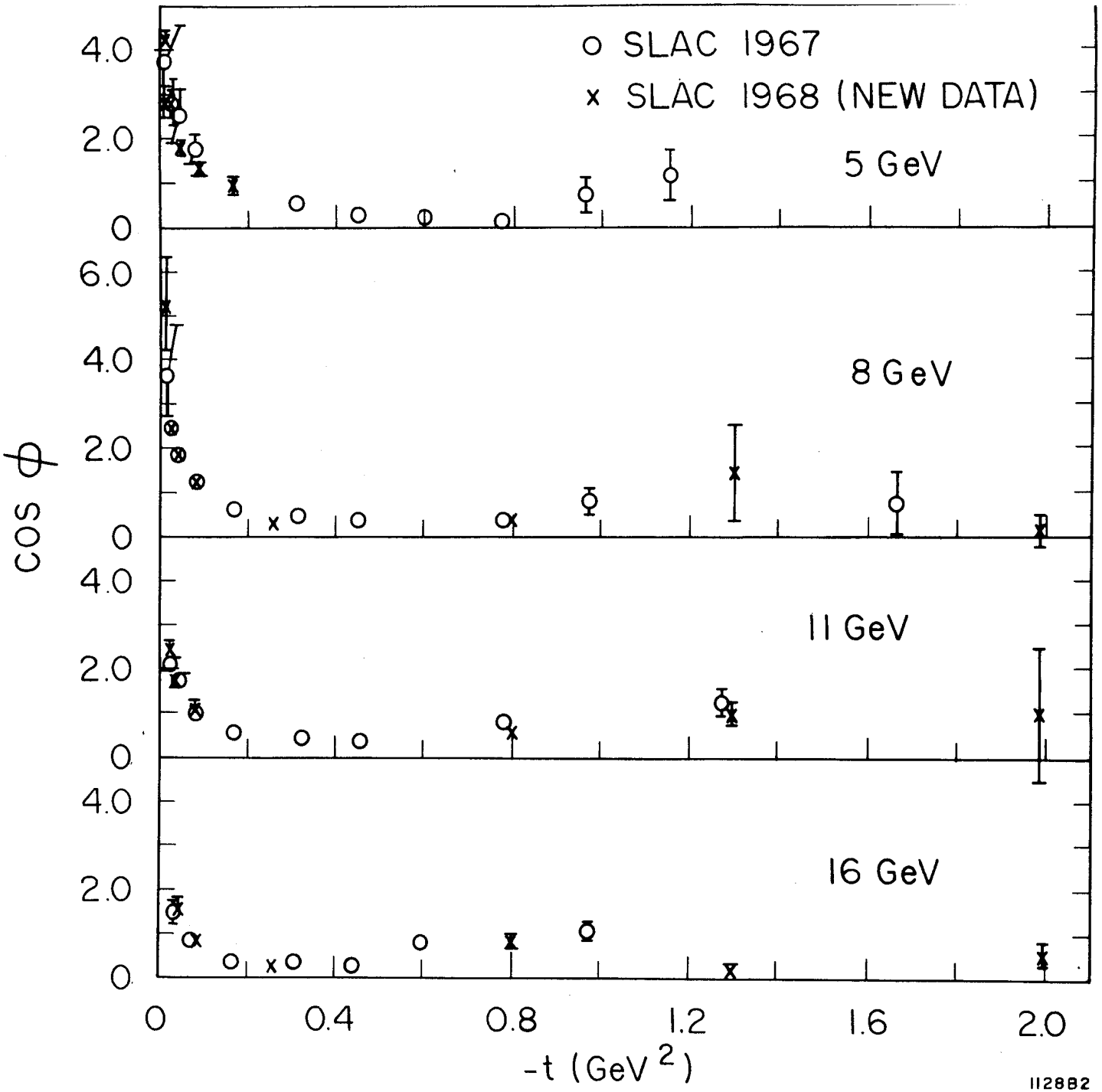
o SLAC 1967
x SLAC 1968 (NEW DATA)
5 GeV
8 GeV
11 GeV
16 GeV
cos φ
-t (GeV 2)
4.0
2.0
0
6.0
0.4
0.8
1.2
1.6
2.0
112882

Fig. 30

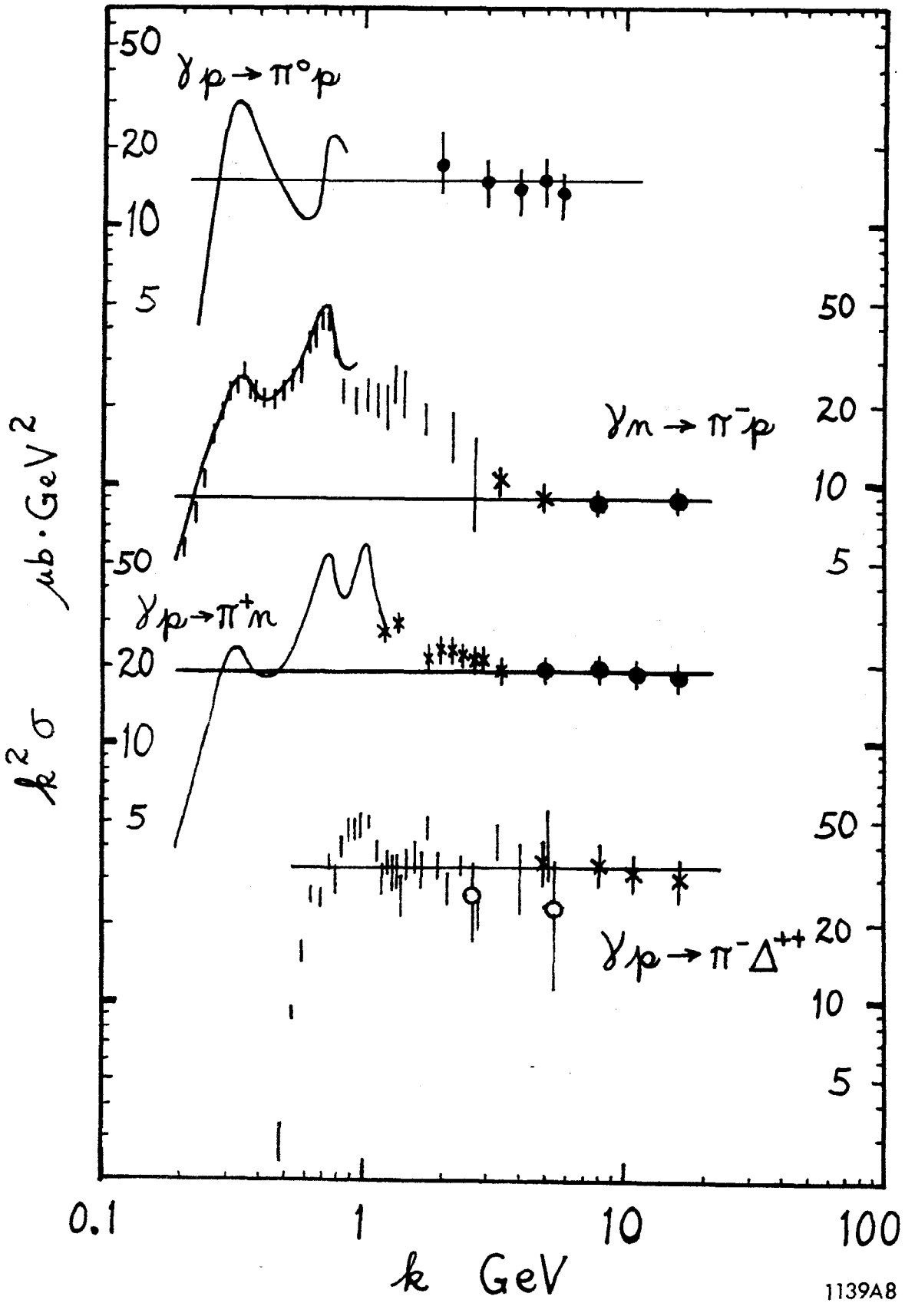
$\gamma p \to \pi^0 p$
$\gamma n \to \pi^- p$
$\gamma p \to \pi^+ n$
$\gamma p \to \pi^- \Delta^{++}$
$k^2\sigma$ $\mu b \cdot GeV^2$
k GeV
0.1
1
10
100
50
20
10
5
1139A8

Fig. 31

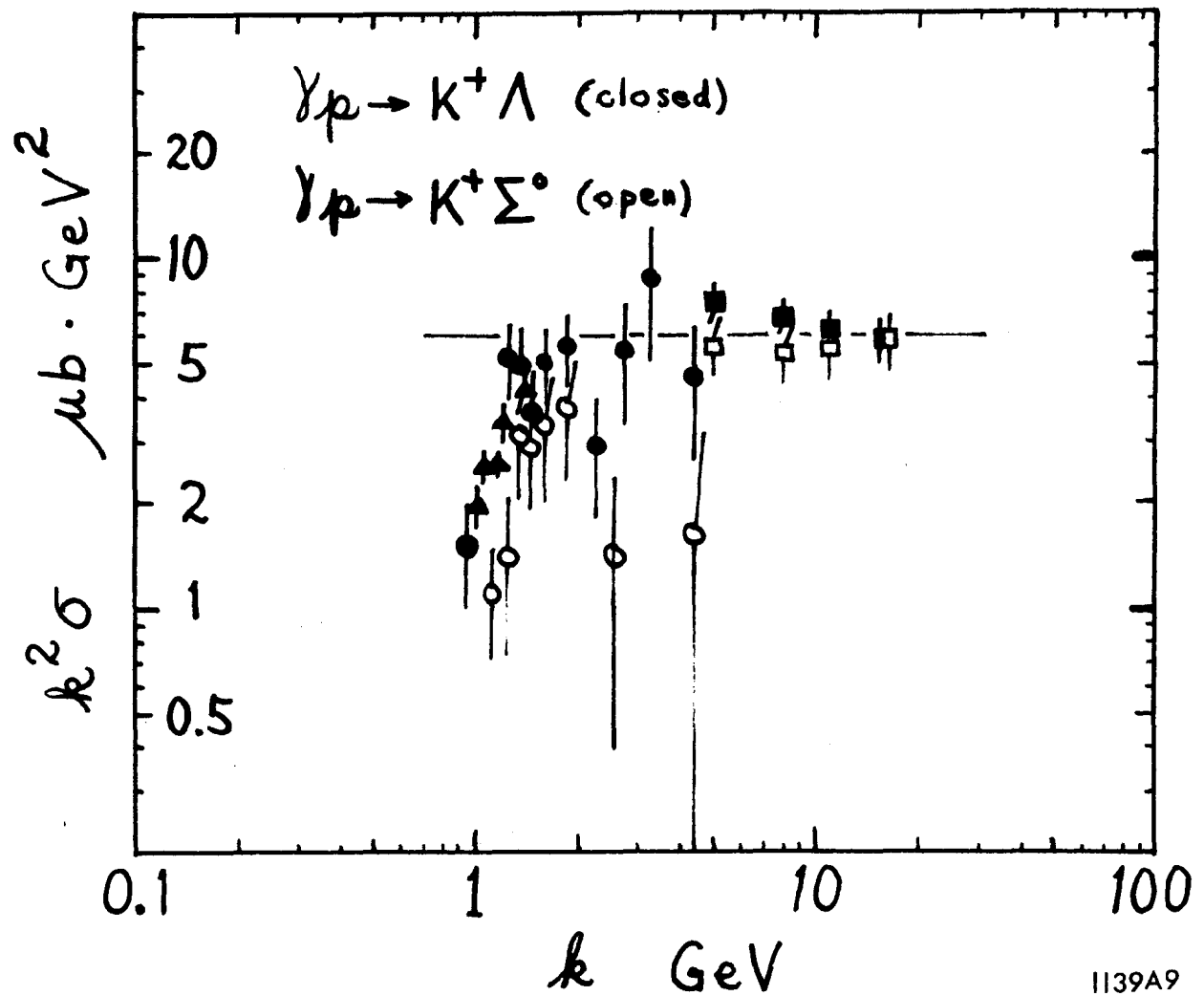
γp → K⁺Λ (closed)
γp → K⁺Σ° (open)
k²σ μb · GeV²
20
10
5
2
1
0.5
0.1
1
10
100
k GeV
1139A9

Fig. 32